UNCLASSIFIED

AD NUMBER
AD909763
LIMITATION CHANGES
TO: Approved for public release; distribution is unlimited.
FROM: Distribution authorized to U.S. Gov't. agencies only; Test and Evaluation; APR 1973. Other requests shall be referred to Air Force Armament Lab., Eglin AFB, FL.
AUTHORITY
AFAL ltr 30 Aug 1973

THIS PAGE IS UNCLASSIFIED

AEDC-TR-73-84 MAY 16 1973

AFATL-TR-73-100

Cy 2

STATIC STABILITY AND DRAG CHARACTERISTICS OF A LOW COST FULL-SCALE TARGET AT MACH NUMBERS FROM 0.2 TO 1.3

J. B. Carman

ARO, Inc.

April 1973

This docu... release

Per TAB 76-4
13 Feb, 1976

PROPULSION WIND TUNNEL FACILITY
ARNOLD ENGINEERING DEVELOPMENT CENTER
AIR FORCE SYSTEMS COMMAND
ARNOLD AIR FORCE STATION, TENNESSEE

NOTICES

STATIC STABILITY AND DRAG CHARACTERISTICS OF A LOW COST FULL-SCALE TARGET AT MACH NUMBERS FROM 0.2 TO 1.3

J. B. Carman
ARO, Inc.

FOREWORD

The work reported herein was conducted by the Arnold Engineering Development Center (AEDC) and sponsored by the Air Force Armament Laboratory (AFATL/DLQC), Air Force Systems Command (AFSC), under Program Element 62602F, Project 1920.

The test results presented were obtained by ARO, Inc. (a subsidiary of Sverdrup & Parcel and Associates, Inc.), contract operator of AEDC, AFSC, Arnold Air Force Station, Tennessee. The test was conducted from February 12 through 14, 1973, under ARO Project No. PA282. The manuscript was submitted for publication on April 11, 1973.

This technical report has been reviewed and is approved.

L. R. KISSLING	A. L. COAPMAN
Lt Colonel, USAF	Colonel, USAF
Chief Air Force Test Director, PWT	Director of Test
Directorate of Test	

ABSTRACT

The static stability and drag characteristics were investigated for a 0.05-scale model of a Low Cost Full-Scale Target (LCFST) at Mach numbers from 0.2 to 1.3. Free-stream Reynolds number, based on the mean aerodynamic chord, varied between 0.9 and 2.2 million for angles of attack and sideslip of -2 to 8 deg and -3 to 3 deg, respectively. Data were obtained for horizontal tail deflections of -0.5 and -2 deg. Test results indicated that the target vehicle was statically stable in both the pitch and yaw planes. Negative deflection of the horizontal tail produced a substantial increase in pitching-moment coefficient at $\alpha = 0$.

CONTENTS

		Page
	ABSTRACT	iii
	NOMENCLATURE	vi
I.	INTRODUCTION	1
II.	APPARATUS	
	2.1 Test Facility	1
	2.2 Test Article	1
	2.3 Instrumentation	1
III.	TEST PROCEDURE	
	3.1 Test Conditions and Description	2
	3.2 Data Reduction	2
	3.3 Precision of Measurements	2
IV.	RESULTS AND DISCUSSION	
	4.1 Longitudinal Stability and Axial-Force Characteristics	3
	4.2 Lateral Stability and Axial-Force Characteristics	4
	REFERENCES	5

APPENDIXES

I. ILLUSTRATIONS

Figure		
1.	Schematic of the Tunnel 4T Test Section Showing Model Location	9
2.	Model Installation Photographs	10
3.	Model Details	11
4.	Variation of the Longitudinal Stability and Axial-Force Characteristics with Angle of Attack, $\beta = 0$	15
5.	Variation of the Longitudinal Stability Derivatives and Axial-Force Coefficients at Zero Angle of Attack with Mach Number, $\beta = 0$	27
6.	Effects of Horizontal Tail Deflection on the Pitching-Moment and Trim Characteristics, $\beta = 0$	28
7.	Variation of the Lateral Stability and Axial-Force Characteristics with Angle of Sideslip, $\alpha = 0$	29
8.	Variation of the Model Cavity and Base Pressure Ratios with Mach Number	45
9.	Variation of the Lateral Stability Derivatives at Zero Angle of Sideslip with Mach Number, $\alpha = 0$	46

II. TABLES

I.	Wind Tunnel Test Conditions	47
II.	Test Summary	48

NOMENCLATURE

A_b	Model base area, 0.0124 sq ft
C_A	Axial-force coefficient, axial force/$q_\infty S$
$C_{A,B}$	Base axial-force coefficient, $-C_{p_b}(A_b/S)$
$C_{A,F}$	Forebody axial-force coefficient, $C_A - C_{A,B}$
C_ℓ	Rolling-moment coefficient, rolling moment/$q_\infty S\bar{c}$
C_{ℓ_β}	Rolling-moment derivative, $\partial C_\ell/\partial\beta$, per degree
C_m	Pitching-moment coefficient (see Fig. 3 for moment reference location), pitching moment/$q_\infty S\bar{c}$
C_{m_α}	Pitching-moment derivative, $\partial C_m/\partial\alpha$, per degree
C_N	Normal-force coefficient, normal force/$q_\infty S$
C_{N_α}	Normal-force derivative, $\partial C_N/\partial\alpha$, per degree
C_n	Yawing-moment coefficient, yawing moment/$q_\infty S\bar{c}$
C_{n_β}	Yawing-moment derivative, $\partial C_n/\partial\beta$, per degree
C_{p_b}	Base pressure coefficient, $(p_b - p_\infty)/q_\infty$
C_Y	Side-force coefficient, side force/$q_\infty S$
C_{Y_β}	Side-force derivative, $\partial C_Y/\partial\beta$, per degree
$\bar{c}$	Reference length, theoretical mean aerodynamic chord, 0.7 ft
M_∞	Free-stream Mach number
p_b	Model base pressure, psfa
p_{CAV}	Model cavity pressure (forward of inlets), psfa
p_t	Free-stream total pressure, psfa
p_∞	Free-stream static pressure, psfa

q_∞	Free-stream dynamic pressure, psfa
Re_ℓ	Free-stream Reynolds number based on model reference length
S	Reference area, theoretical wing area, 0.625 sq ft
T_t	Free-stream total temperature, °R
α	Model angle of attack, deg
α_t	Model trim angle of attack, deg
β	Model angle of sideslip, deg
δ_e	Horizontal tail deflection, positive trailing edge down, deg

SECTION I
INTRODUCTION

The purpose of the present investigation was to determine the aerodynamic characteristics of a Low Cost Full-Scale Target (LCFST) vehicle at subsonic and transonic Mach numbers. The tests were conducted in the Aerodynamic Wind Tunnel (4T) at Mach numbers from 0.2 to 1.3 using a 0.05-scale model. Reynolds number based on the mean aerodynamic chord varied between 0.9 and 2.2 million for angles of attack from -2 to 8 deg and angles of sideslip from -3 to 3 deg. Values of horizontal tail deflection angle were -0.5 and -2 deg.

SECTION II
APPARATUS

2.1 TEST FACILITY

The Aerodynamic Wind Tunnel (4T) is a closed-loop, continuous flow, variable-density tunnel in which the Mach number can be varied from 0.1 to 1.3. At all Mach numbers, the stagnation pressure can be varied from 300 to 3700 psfa. The test section is 4 ft square and 12.5 ft long with perforated, variable porosity (0.5- to 10-percent open) walls. It is completely enclosed in a plenum chamber from which the air can be evacuated, allowing part of the tunnel airflow to be removed through the perforated walls of the test section. A more thorough description of the tunnel is given in Ref. 1.

2.2 TEST ARTICLE

A schematic drawing of the model installation location in the test section is shown in Fig. 1 (Appendix I). Model photographs and details are shown in Figs. 2 and 3, respectively. The 0.05-scale model (Fig. 3a) was 28.6 in. long and had a wingspan of 15 in. Horizontal tail deflection (δ_e) was either -0.5 or -2 deg, and the inlets for the engine were open to allow flow through the cavity in the model (Fig. 3b). The model was tested both with and without artificial boundary layer trips (No. 100 carborundum grit). The grit was placed on the model in 0.1-in.-wide strips at 1 in. from the nose and at 0.75 in. from the leading edges on both sides of the wings and vertical tail. The model was fabricated from aluminum and furnished by the AFATL/DLQC.

2.3 INSTRUMENTATION

Aerodynamic forces and moments on the model were measured with a six-component, moment-type, internal strain-gage balance supplied and calibrated by the Propulsion Wind Tunnel Facility (PWT). Model base pressures were measured with 5-psid transducers.

SECTION III
TEST PROCEDURE

3.1 TEST CONDITIONS AND DESCRIPTION

A complete test summary and the wind tunnel test conditions are given in the tables of Appendix II. Steady-state force data were obtained at nominal free-stream Mach numbers of 0.2 to 1.3 in 0.05 increments. Tunnel conditions were held constant at each Mach number while pitch or yaw angle was varied and data recorded at each selected angle. The pitch and yaw ranges were from -2 to 8 deg and -3 to 3 deg, respectively. Horizontal tail deflection angles were -0.5 and -2 deg. Artificial boundary layer trips were applied only for that portion of the test with δ_e = -0.5 deg.

3.2 DATA REDUCTION

Force and moment data were reduced to coefficient form in the body axis coordinate system. The moment reference was 16.25 in. aft of the model nose and located on the engine centerline.

3.3 PRECISION OF MEASUREMENTS

Uncertainties in the basic tunnel parameters, p_t, T_t, and M_∞ were estimated from repeat calibrations of the instrumentation and from repeatability and uniformity of the test section flow during tunnel calibration. These uncertainties were then used to estimate the uncertainties in other free-stream properties, using the Taylor series method of error propagation (Ref. 2).

Free-Stream Mach Number	Uncertainty, percent					
	M_∞	p_t	T_t	p_∞	q_∞	Re_ℓ
0.20	±1.0	±0.1	±0.4	±0.1	±2.0	±1.1
0.25	±0.9				±1.6	±1.0
0.30	±0.7				±1.3	±0.8
0.35	±0.6				±1.1	±0.8
0.40	±0.5			±0.2	±1.0	±0.7
0.45	±0.5	±0.2			±0.8	
0.50	±0.4				±0.7	
0.55				±0.3	±0.7	±0.6
0.60					±0.6	
0.65	±0.3	±0.3			±0.5	
0.70				±0.4		±0.7
0.75						
0.80						
0.85				±0.5		
0.90		±0.4		±0.5		
0.95				±0.6		
1.00	±0.4			±0.6		
1.05	±0.5			±0.7		
1.10	±0.5			±0.9		
1.15	±0.7			±1.1		
1.20	±0.8			±1.3	±0.6	
1.25	±0.9	±0.5		±1.6		±0.8
1.30	±1.1	±0.5		±2.0		±0.8

Model attitude corrections were made for model-balance deflections under airload. The precision of angle of attack is estimated to be ±0.1 deg.

The balance uncertainties, based on a 95-percent confidence level, were combined with the uncertainties in the tunnel parameters, assuming a Taylor series error propagation, to estimate the precision of the aerodynamic coefficients. The maximum estimated uncertainties are given as follows:

Free-Stream Mach Number	Uncertainty					
	C_N	C_m	C_Y	C_n	C_ℓ	$C_{A,F}$
0.20	±0.011	±0.0007	±0.002	±0.0007	±0.0006	±0.004
0.25	±0.009	±0.0007	±0.002	±0.0007	±0.0006	±0.003
0.30	±0.007	±0.0005	±0.001	±0.0005	±0.0004	±0.002
0.35	±0.005	±0.0004	↓	±0.0004	±0.0003	↓
0.40	±0.004	↓	↓	↓	↓	↓
0.45	↓	↓	↓	↓	↓	↓
0.50	↓	↓	↓	↓	↓	↓
0.55	±0.003	↓	↓	↓	↓	↓
0.60	↓	↓	↓	↓	↓	↓
0.65	↓	↓	↓	↓	↓	↓
0.70	↓	↓	↓	↓	↓	↓
0.75	±0.002	↓	↓	↓	↓	↓
0.80	↓	↓	↓	↓	↓	↓
0.85	↓	↓	↓	↓	↓	↓
0.90	±0.003	↓	↓	↓	↓	↓
0.95	↓	±0.0006	↓	↓	↓	↓
1.00	↓	±0.0008	↓	±0.0005	±0.0004	↓
1.05	↓	±0.0005	↓	↓	↓	±0.001
1.10	↓	±0.0007	↓	↓	↓	↓
1.15	±0.002	±0.0005	↓	↓	↓	↓
1.20	±0.001	↓	↓	↓	↓	↓
1.25	±0.002	↓	↓	↓	↓	±0.002
1.30	±0.002	↓	↓	↓	↓	±0.002

SECTION IV
RESULTS AND DISCUSSION

4.1 LONGITUDINAL STABILITY AND AXIAL-FORCE CHARACTERISTICS

The variations in the longitudinal stability and axial-force characteristics with angle of attack are presented in Fig. 4. Deflecting the horizontal tail from -0.5 to -2 deg produced little change in the normal-force coefficient variations with angle of attack (Fig. 4a) but resulted in a substantial increase in the level of the pitching-moment coefficient (Fig. 4b) as would be expected. Differences in the levels of the axial-force coefficients over the angle-of-attack range are quite evident for the two horizontal tail deflection angles (Fig. 4c). However, these differences should not be attributed to the change in deflection angle (which should produce an insignificant change in $C_{A,F}$) but rather to differences in laminar and turbulent skin friction induced by the artificial boundary layer trips which were applied for δ_e = -0.5 only. It should also be noted that the $C_{A,F}$ values include a component of internal axial force resulting from flow through the inlets.

For $\alpha = 0$, the variation of the longitudinal stability derivatives and axial-force coefficients with Mach number are shown in Fig. 5. A negative increase in horizontal tail deflection angle resulted in little change in C_{N_α} over the Mach number range but produced a slightly more negative C_{m_α}. The differences in C_{m_α} are attributable to nonlinearities in the C_m versus angle-of-attack curves at small angle of attack. This would suggest an effect of the wing wake on the flow about the horizontal stabilizer. Differences in the axial-force coefficients for the model with and without trips decreased sharply for $M_\infty > 0.9$. Since the Reynolds number is too low for transition to move forward naturally, it could be induced by shock separation. As shock separation would reduce the "wetted" area affected by the grit, it is a likely cause for the decreasing difference in the axial-force coefficients at $M_\infty = 0.95$ and 1.0.

The horizontal tail effectiveness along with trim characteristics are presented in Fig. 6. At $\alpha = 0$, a negative increase in horizontal tail deflection angle produced a significant increase in the pitching-moment coefficient over the entire Mach number range. For a horizontal tail deflection angle of -0.5 deg, the model trimmed near $\alpha = 4$ deg for $M_\infty \leq 0.95$, but trim angle dropped sharply to near $\alpha = 0$ for $M_\infty \geq 1.0$. For $\delta_e = -2$ deg, trim angle of attack was higher than the range of angles of attack for the present tests except at $M_\infty = 1.0$ where α_t was approximately 3 deg.

4.2 LATERAL STABILITY AND AXIAL-FORCE CHARACTERISTICS

The variation in the lateral stability and axial-force coefficients with angle of sideslip are shown in Fig. 7. An examination of these data reveals that the values of C_Y (Fig. 7a), C_n (Fig. 7b), and C_ℓ (Fig. 7c) vary linearly with changing sideslip angle and generally do not approach zero at $\beta = 0$, whereas $C_{A,F}$ (Fig. 7d) is relatively constant for different β. In an effort to clarify the former results, the data obtained at $\alpha = 0$, $\beta = 0$ during the pitch angle variations are shown on the figures. Since the C_ℓ data at $\beta = 0$ from the pitch and yaw polars are in good agreement, this would indicate the offset in the C_ℓ curve could probably be attributed to small flow angularity or minor model asymmetry. However, the pitch and yaw polar data for C_Y and C_n at $\beta = 0$ sometimes show large differences, with the pitch data indicating little side force and yawing moment at $\alpha = 0$, $\beta = 0$. At all Mach numbers, the side force necessary to produce the difference in the pitch-yaw C_Y data would have to be located approximately one chord length behind the moment reference to produce the required difference in the C_n data. This suggests that perhaps unsymmetrical flow through the inlet and model cavity influenced the external forces and moments. When the model is rolled to 90 deg (to obtain the yaw data), deflection of the sting-balance from model weight moves the sting closer to the starboard wall of the cavity. Because of this restriction, a high pressure region could occur on this wall, causing a positive side force and negative yawing moment as the data indicate. A phenomenon of this nature would not be observed in the C_ℓ data because of moment reference location nor in the C_Y-C_n pitch plane data where the sting is equidistant from the side walls of the cavity. The cavity pressure data of Fig. 8 tend to support this argument since higher values are obtained at $M_\infty > 1$ where the larger offsets in the C_Y-C_n data also occur. Although the absolute values of the lateral data are apparently in error, the

lateral stability derivatives are quite consistent. As shown in Fig. 9, the lateral derivatives are relatively constant with changing Mach number except near $M_\infty = 1$ where small increases occur.

REFERENCES

1. Test Facilities Handbook (Ninth Edition). "Propulsion Wind Tunnel Facility, Vol. 4." Arnold Engineering Development Center, July 1971.

2. Beers, Yardley. Introduction to the Theory of Error. Addison-Wesley Publishing Company, Inc., Reading, Massachusetts, 1957, pp. 26-36.

APPENDIXES
I. ILLUSTRATIONS
II. TABLES

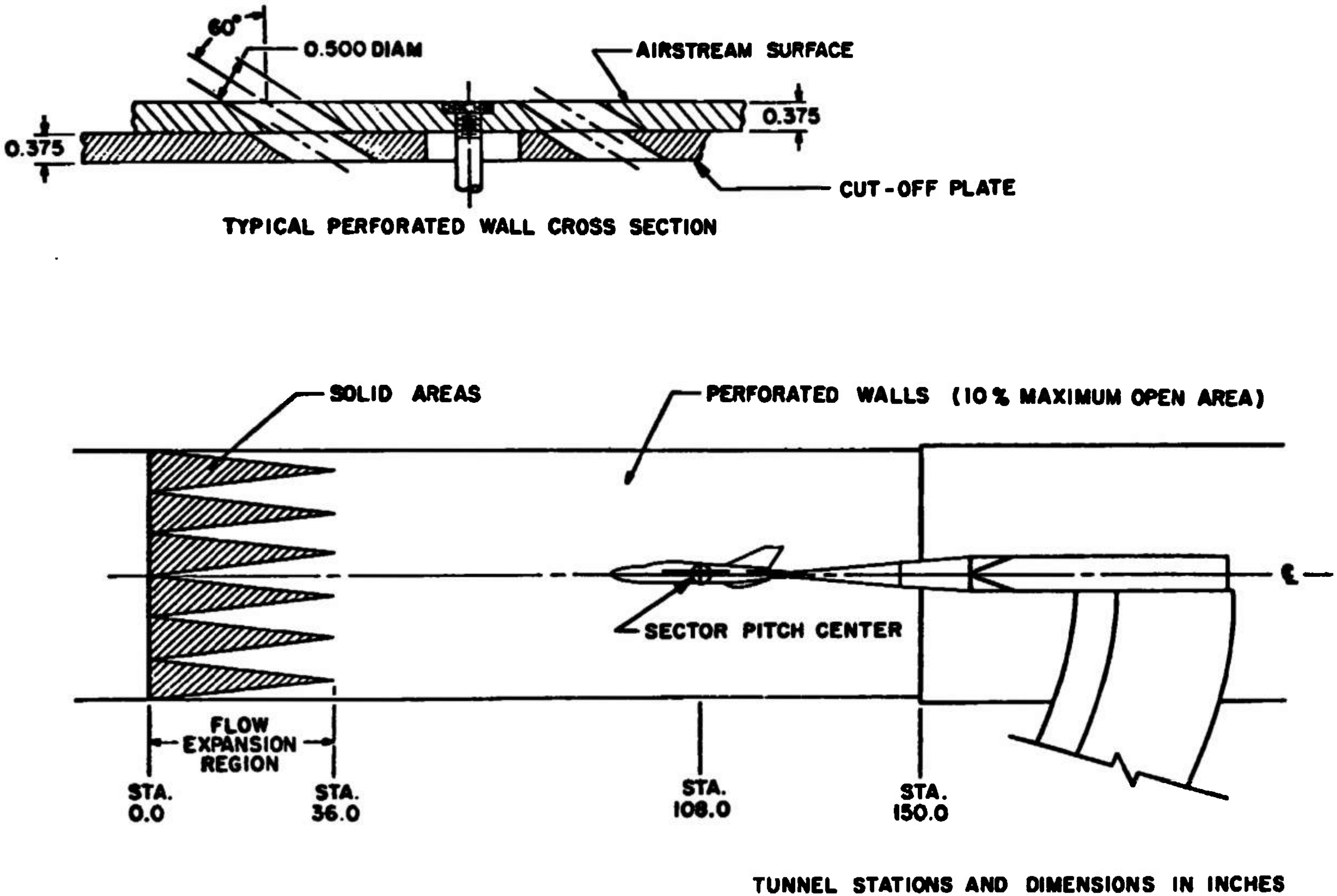

Fig. 1 Schematic of the Tunnel 4T Test Section Showing Model Location

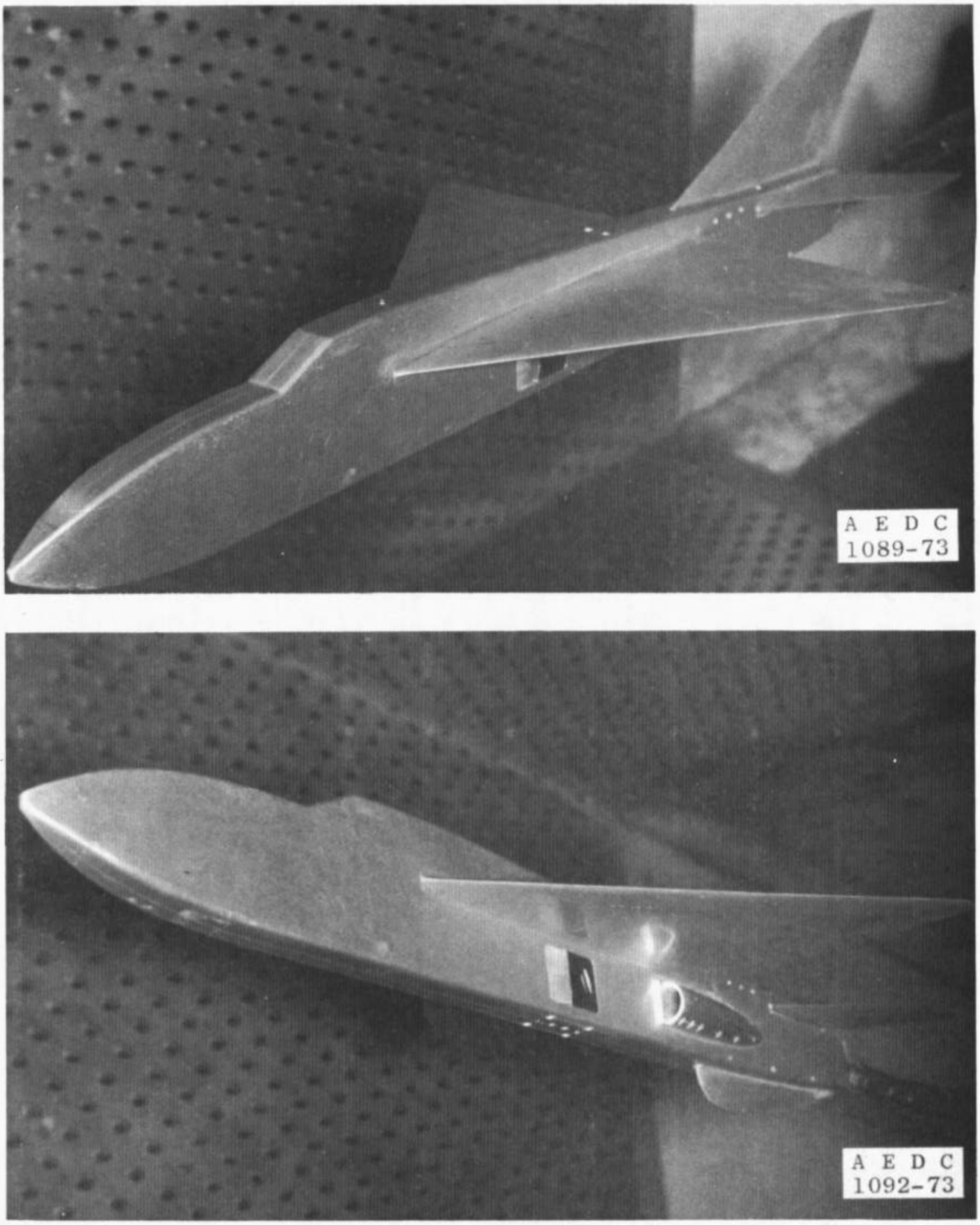

Fig. 2 Model Installation Photographs

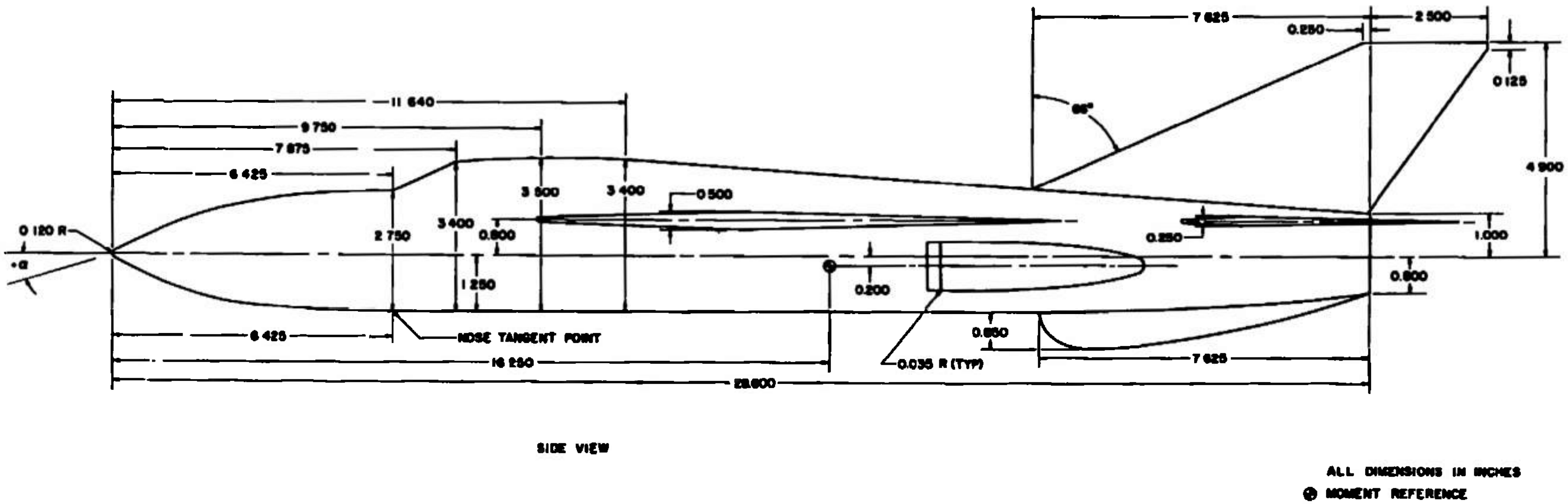

a. Basic Configuration
Fig. 3 Model Details

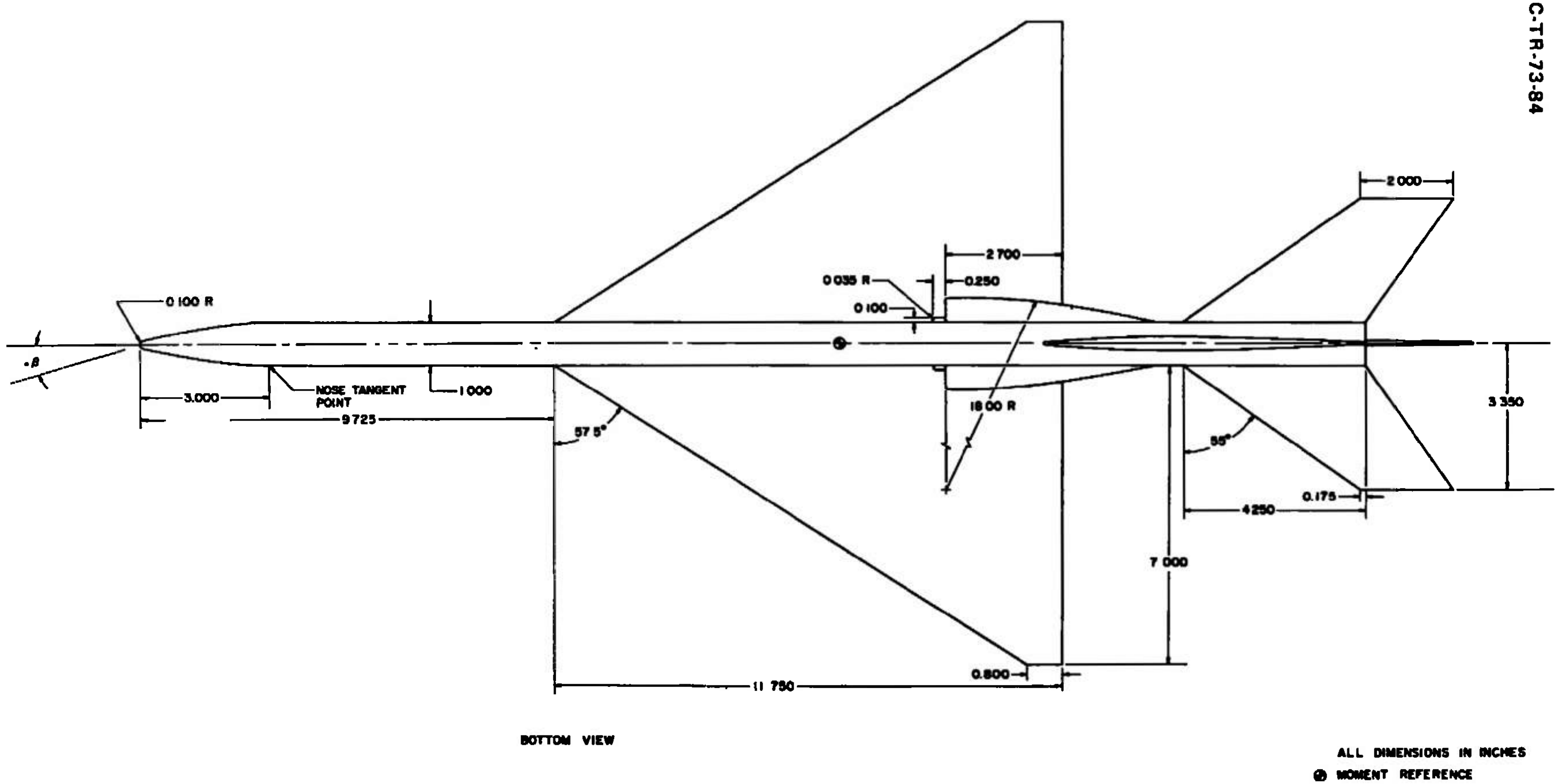

a. Continued
Fig. 3 Continued

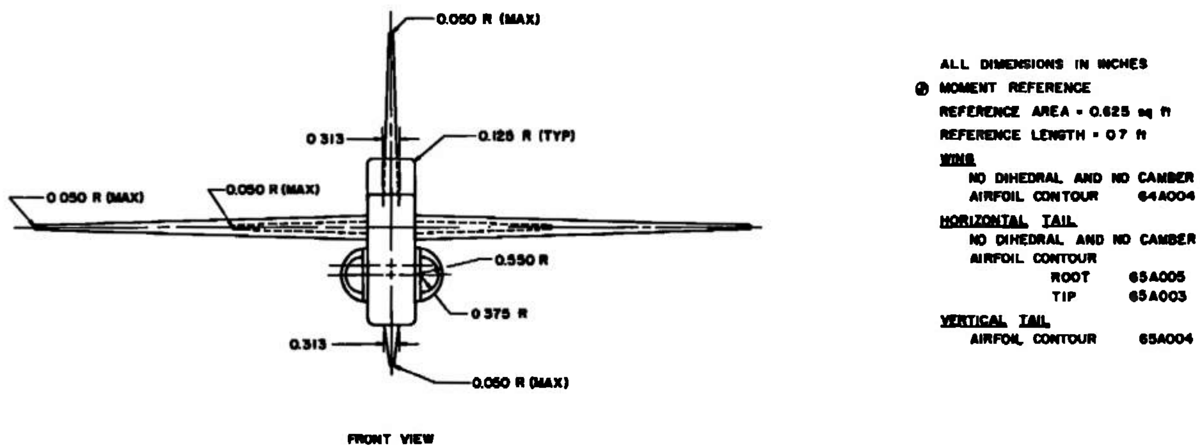

a. Concluded
Fig. 3 Continued

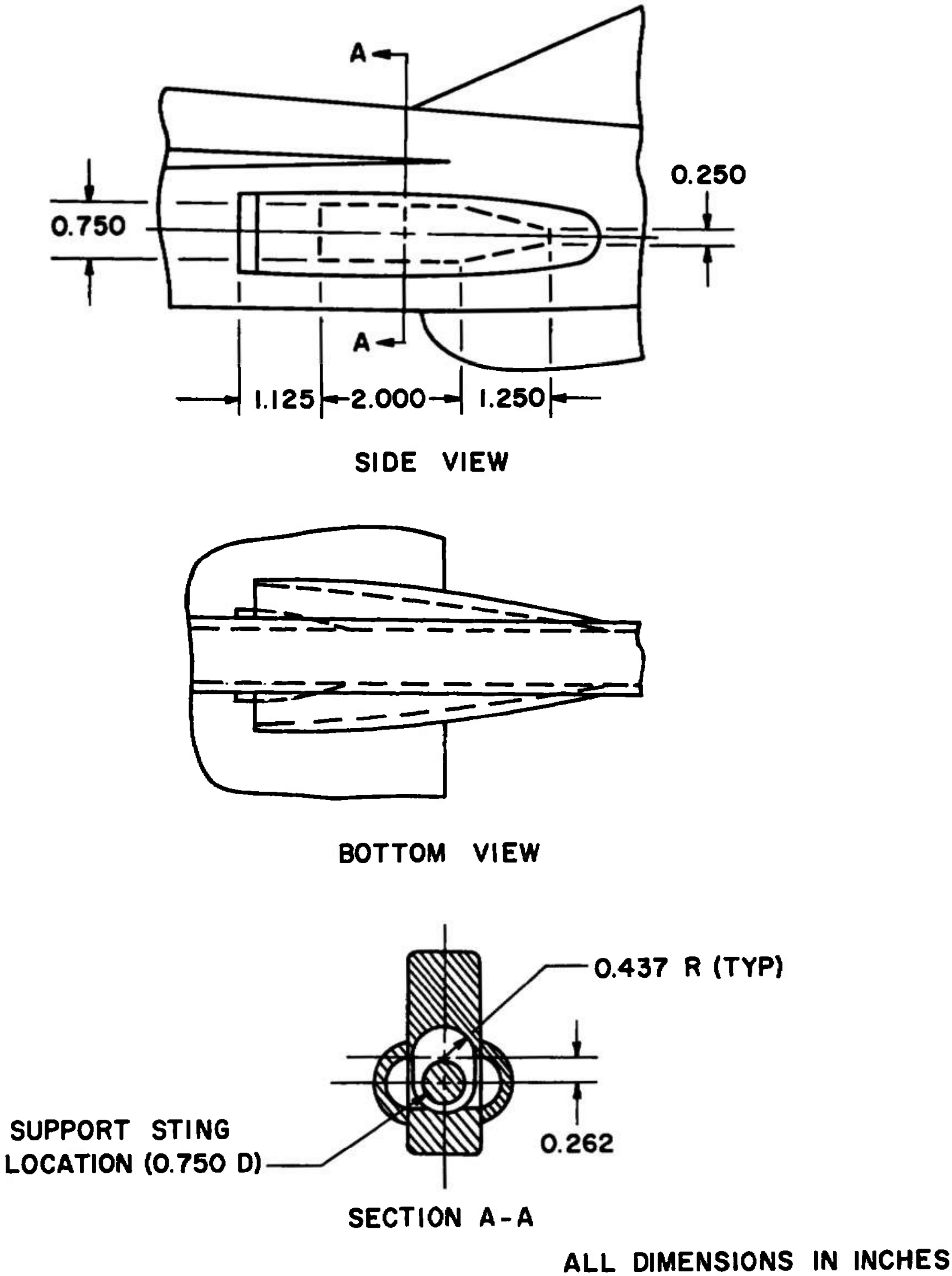

b. Inlet
Fig. 3 Concluded

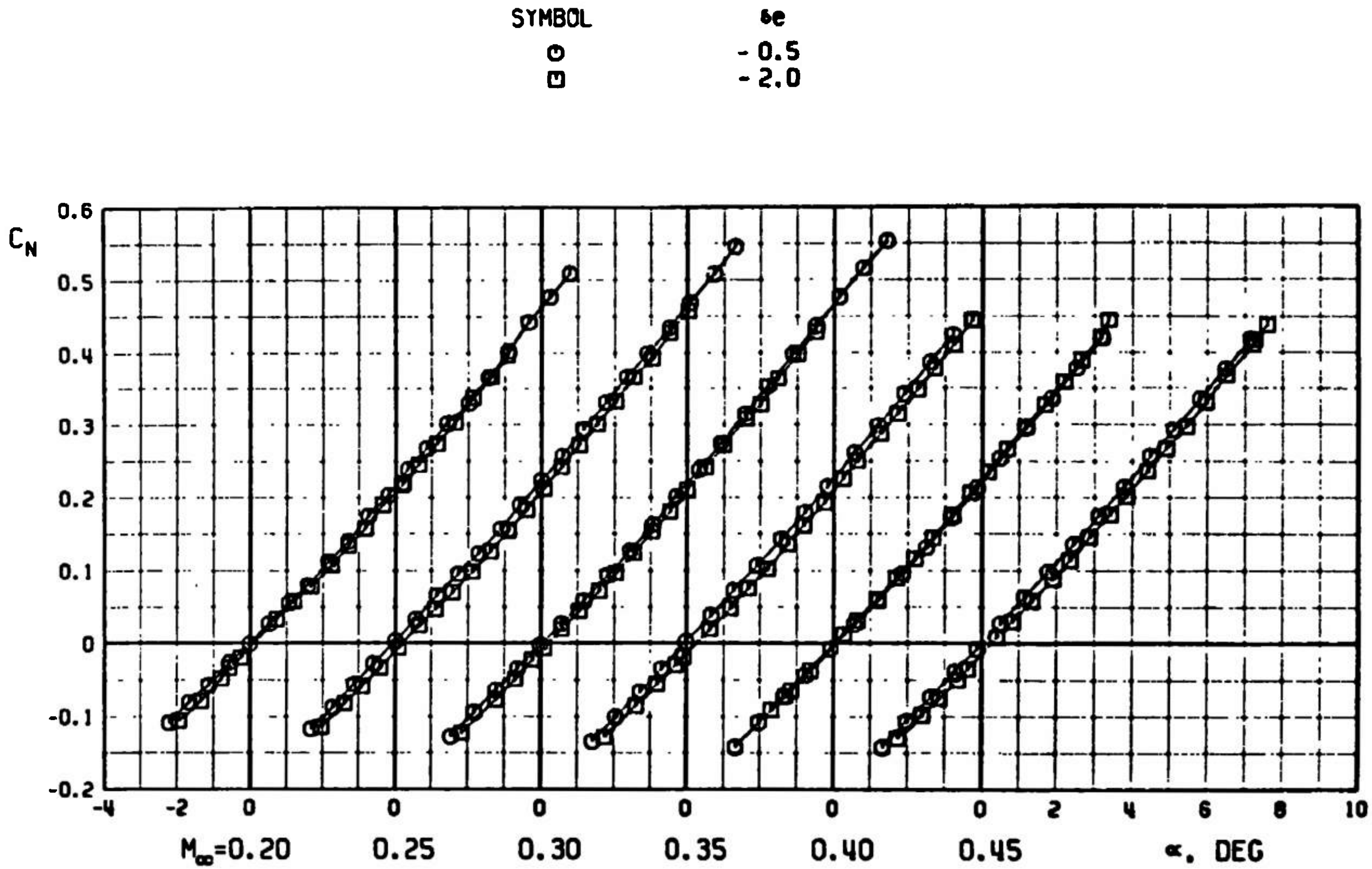

a. C_N versus α

Fig. 4 Variation of the Longitudinal Stability and Axial-Force Characteristics with Angle of Attack, $\beta = 0$

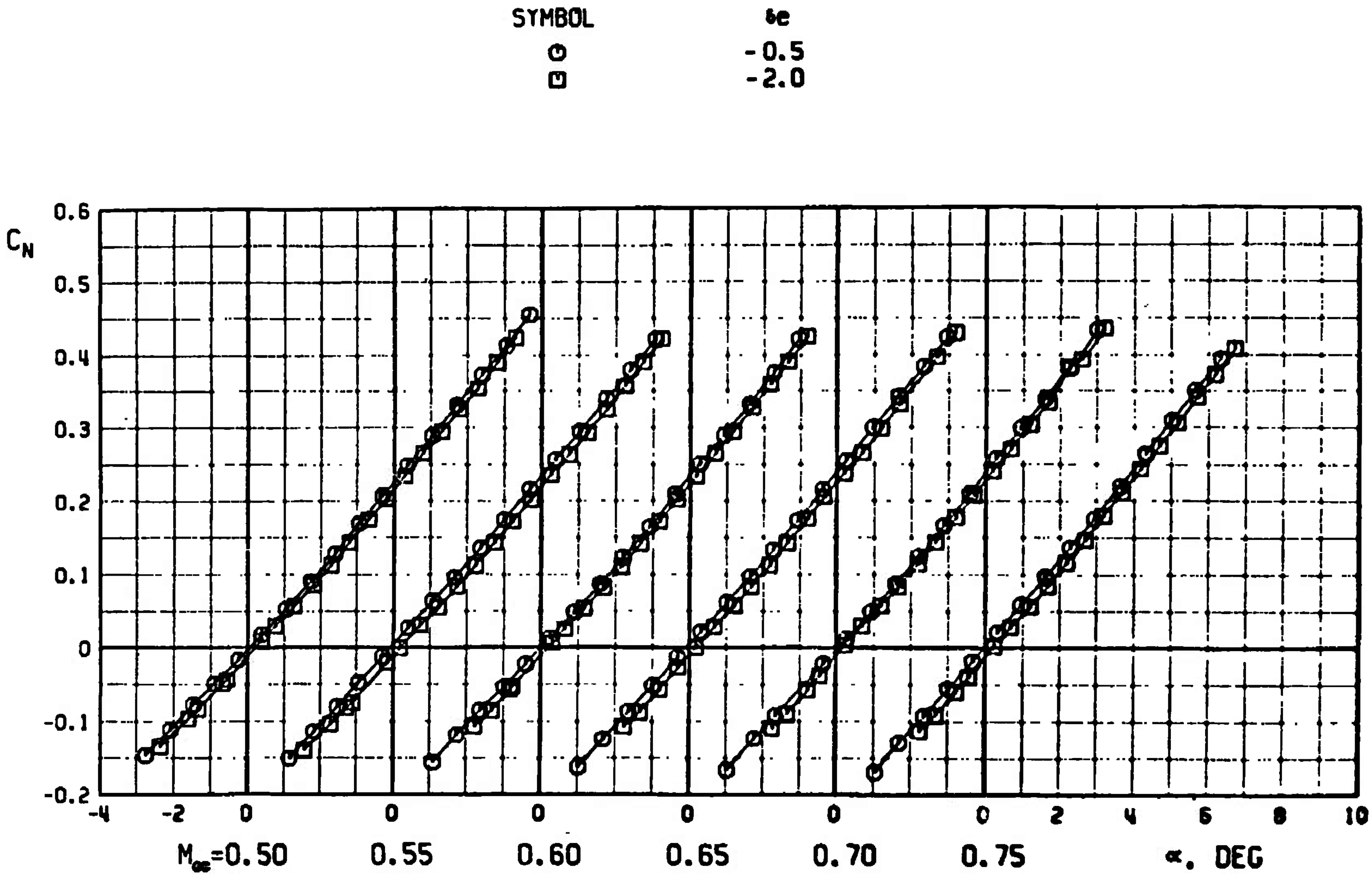

a. Continued
Fig. 4 Continued

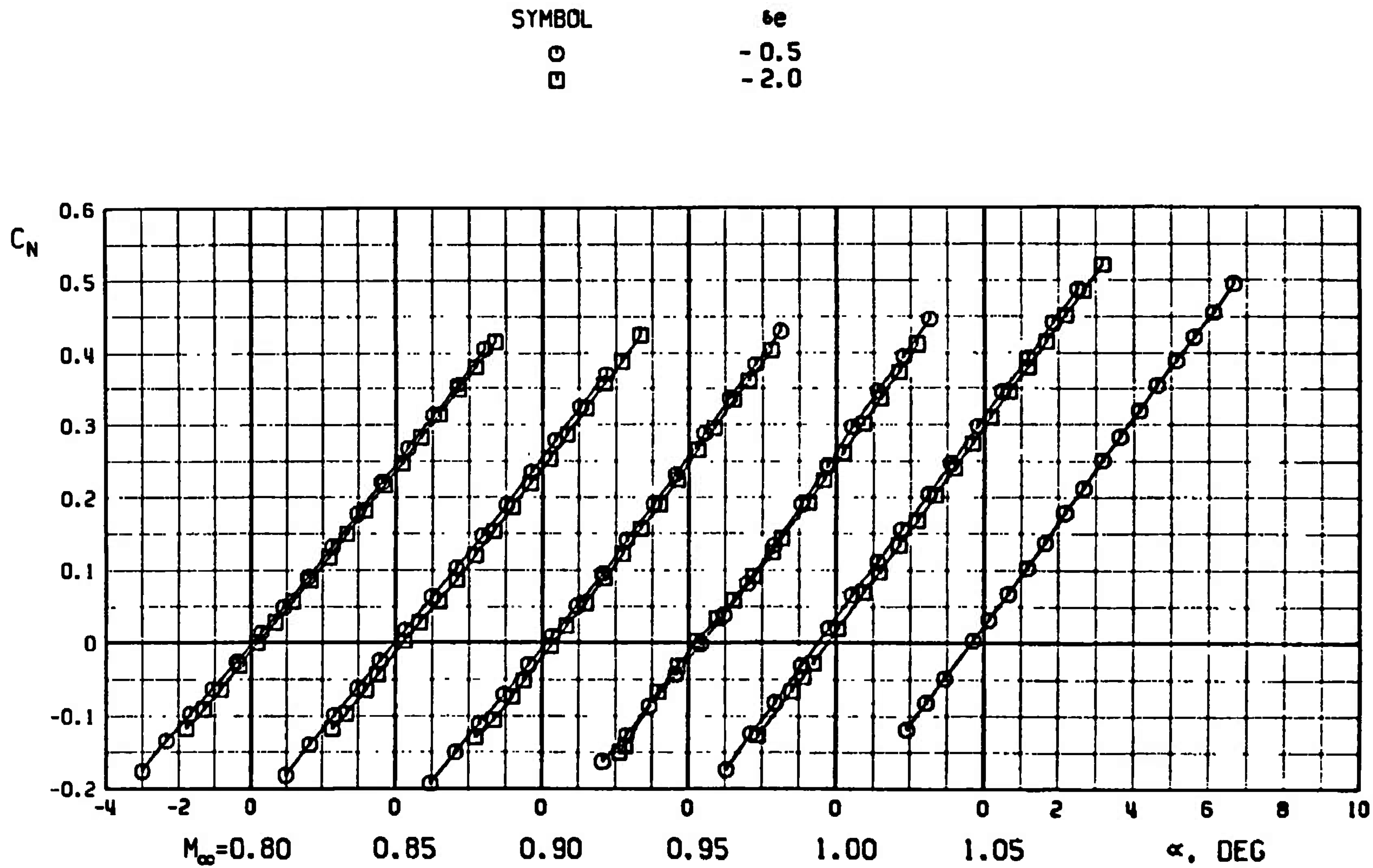

a. Continued
Fig. 4 Continued

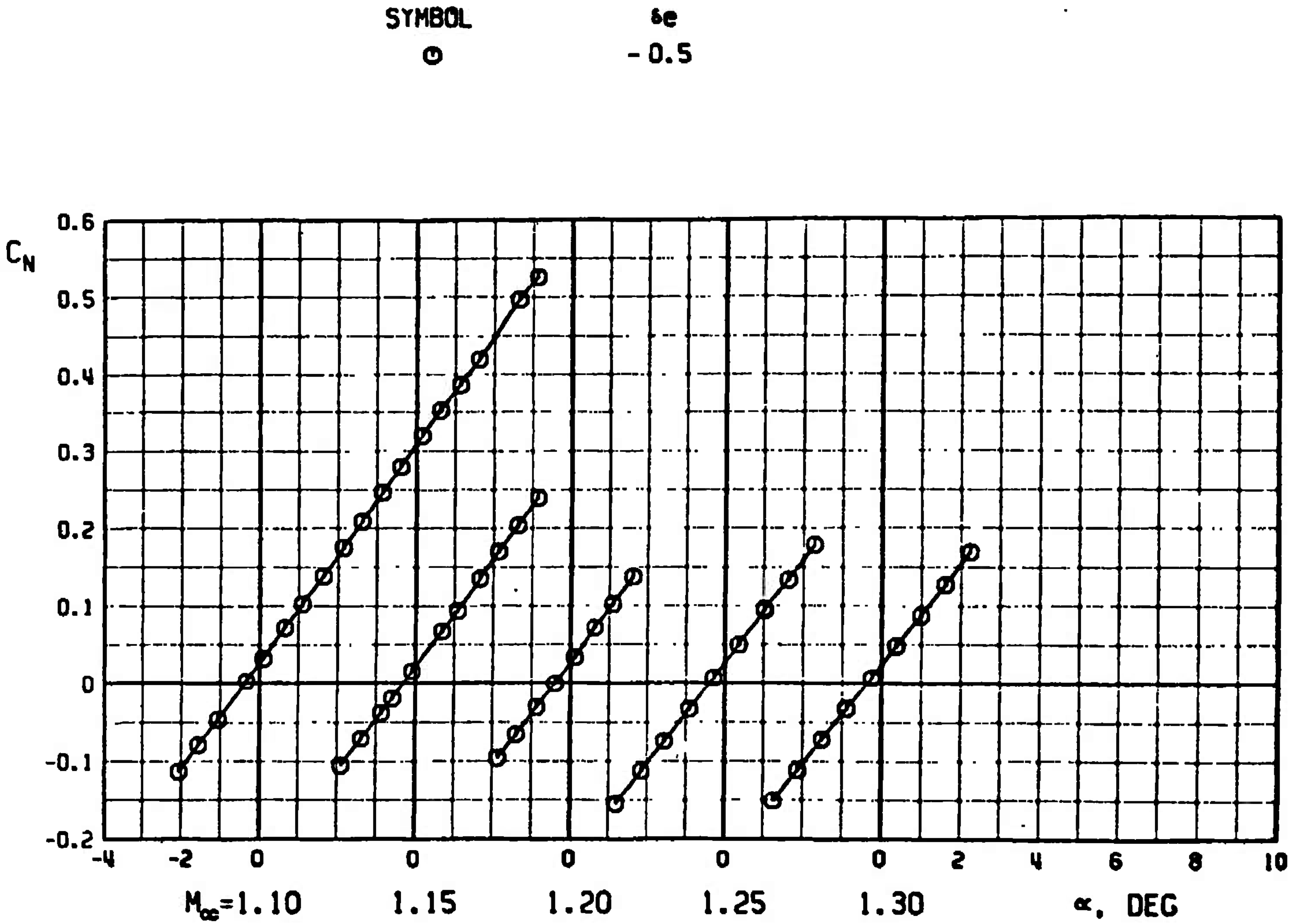

a. Concluded
Fig. 4 Continued

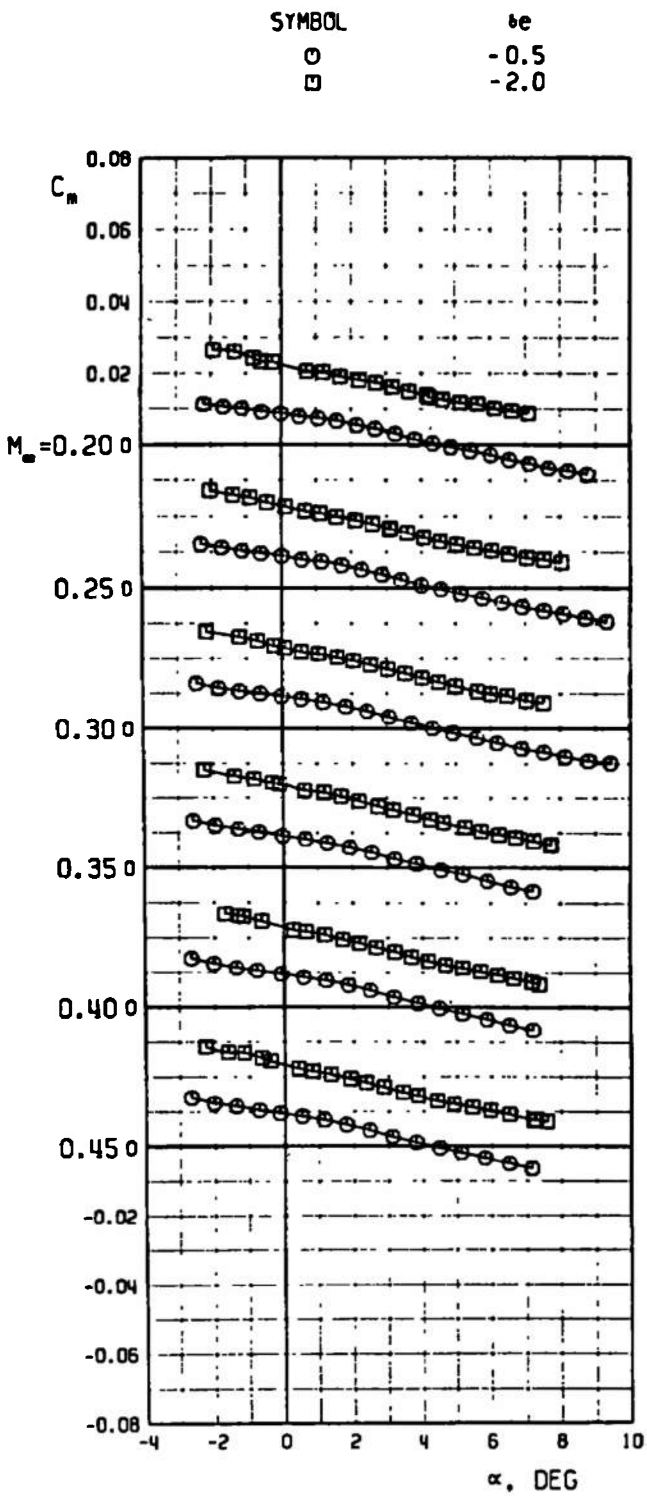

b. C_m versus α
Fig. 4 Continued

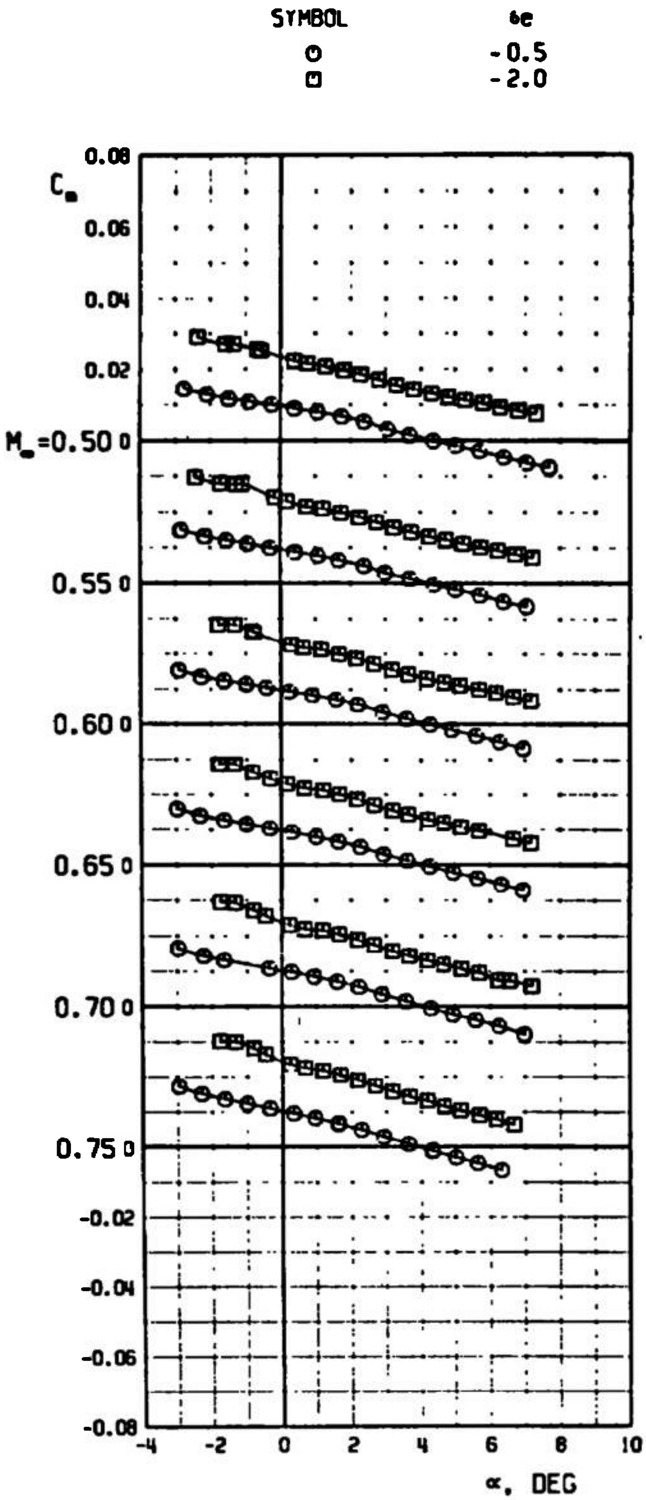

b. Continued
Fig. 4 Continued

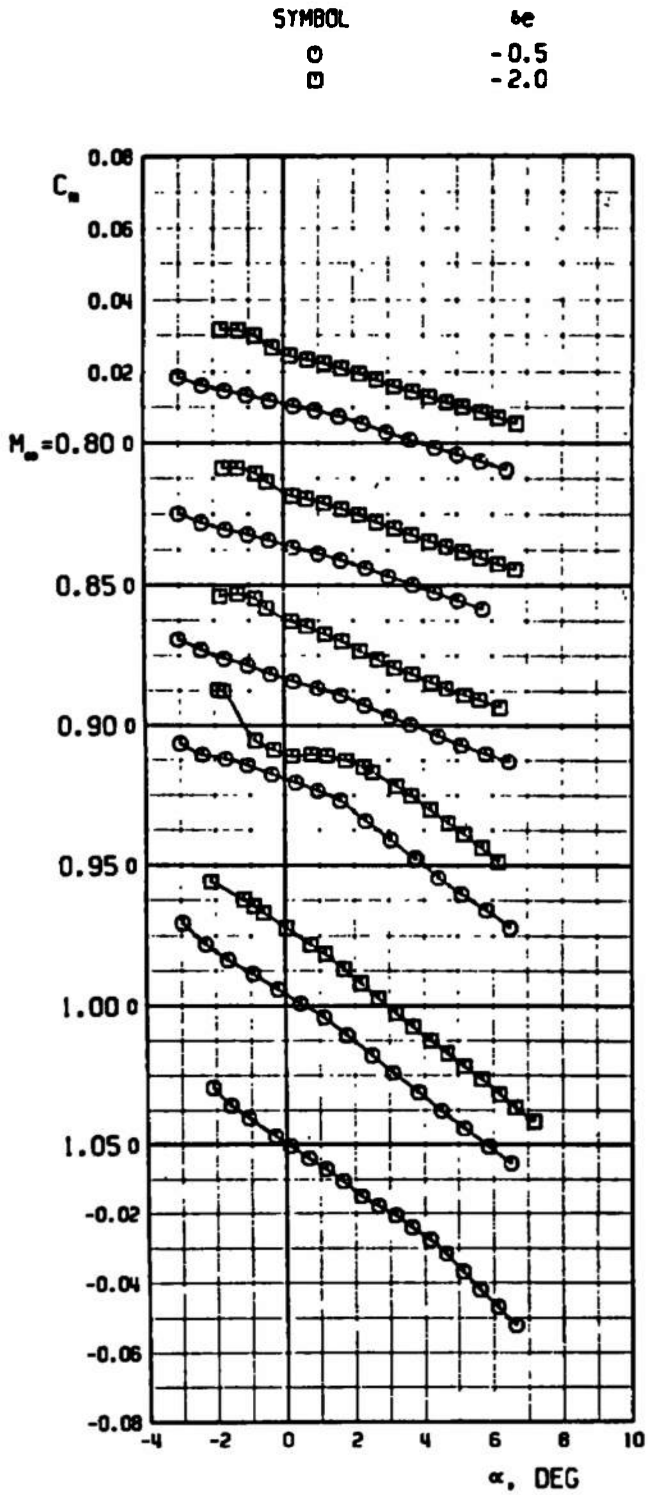

b. Continued
Fig. 4 Continued

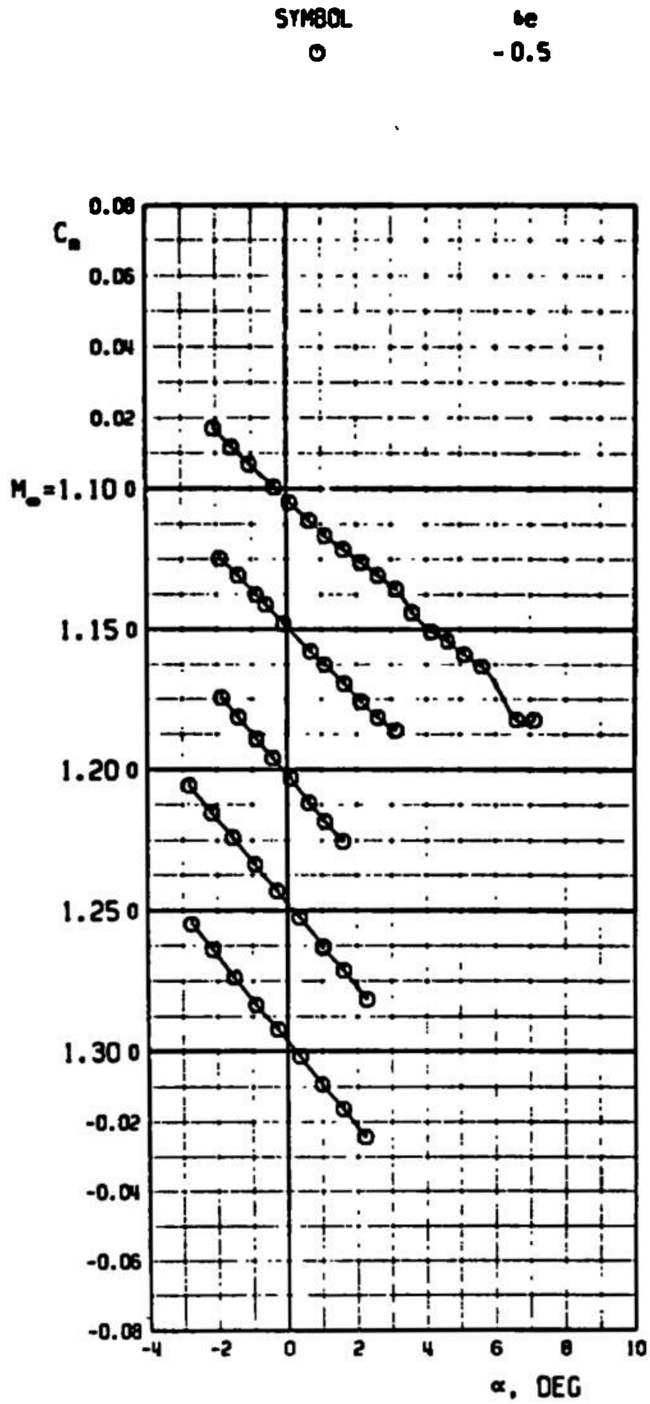

b. Concluded
Fig. 4 Continued

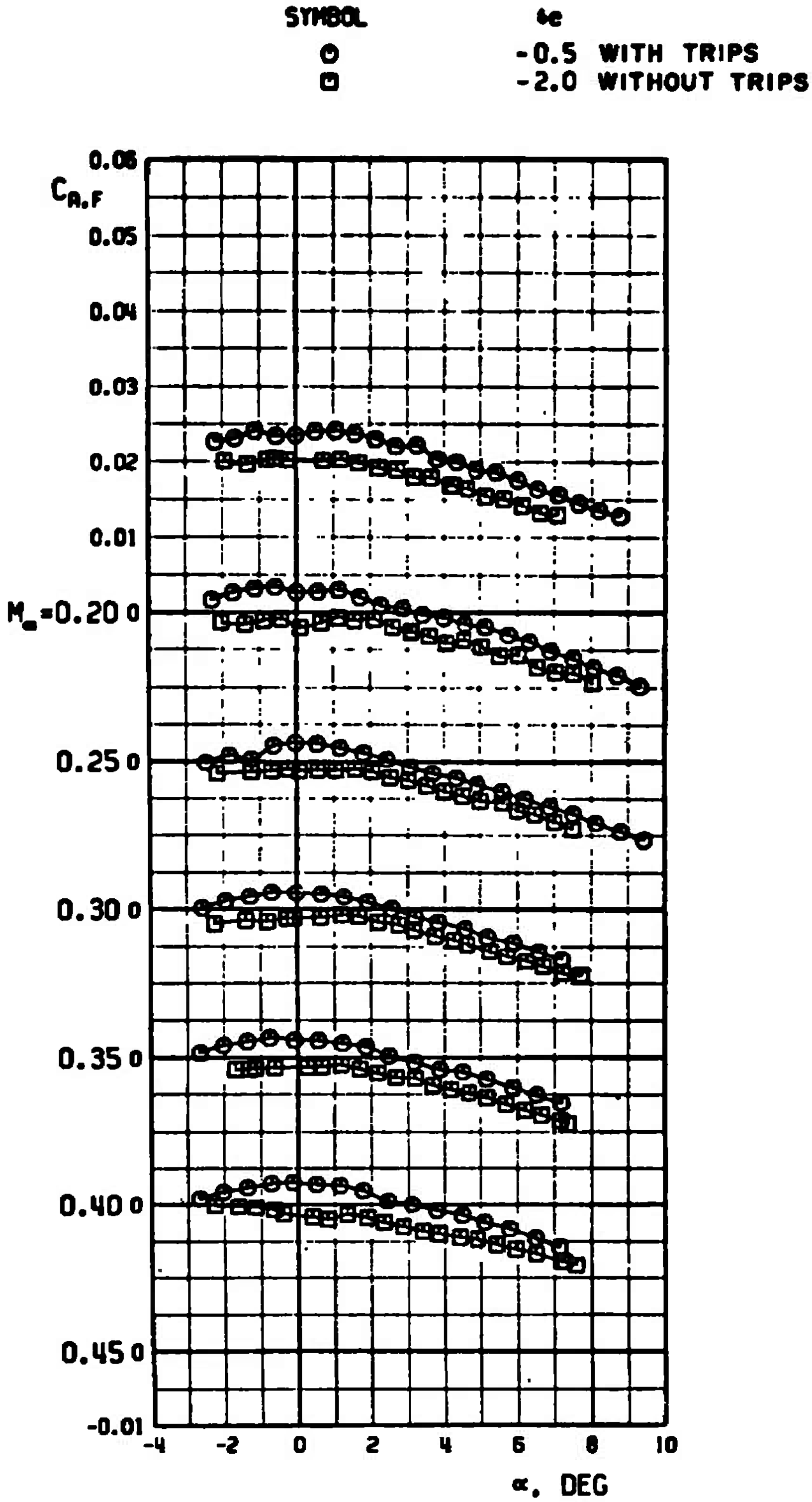

c. $C_{A,F}$ versus α
Fig. 4 Continued

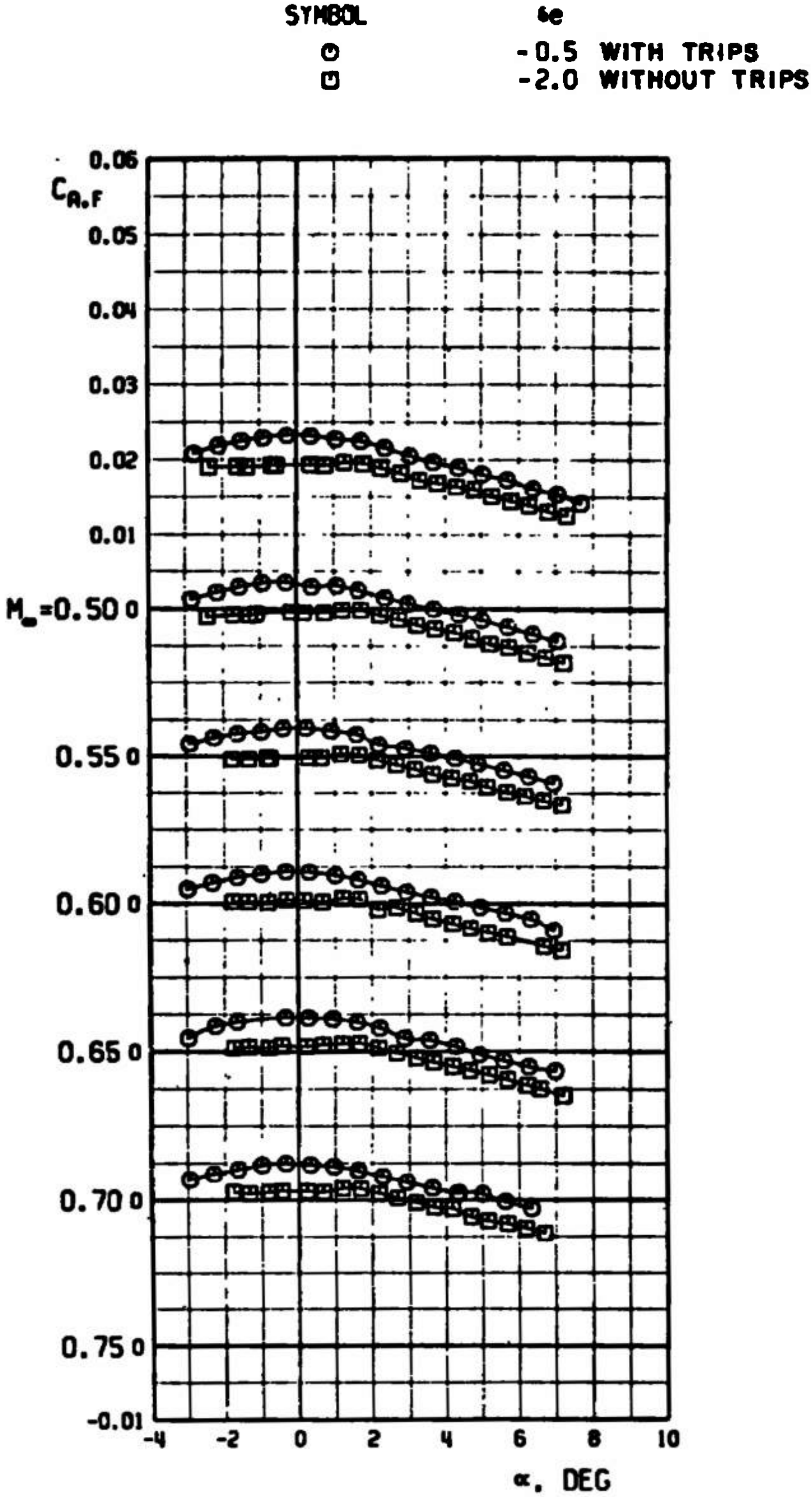

c. Continued
Fig. 4 Continued

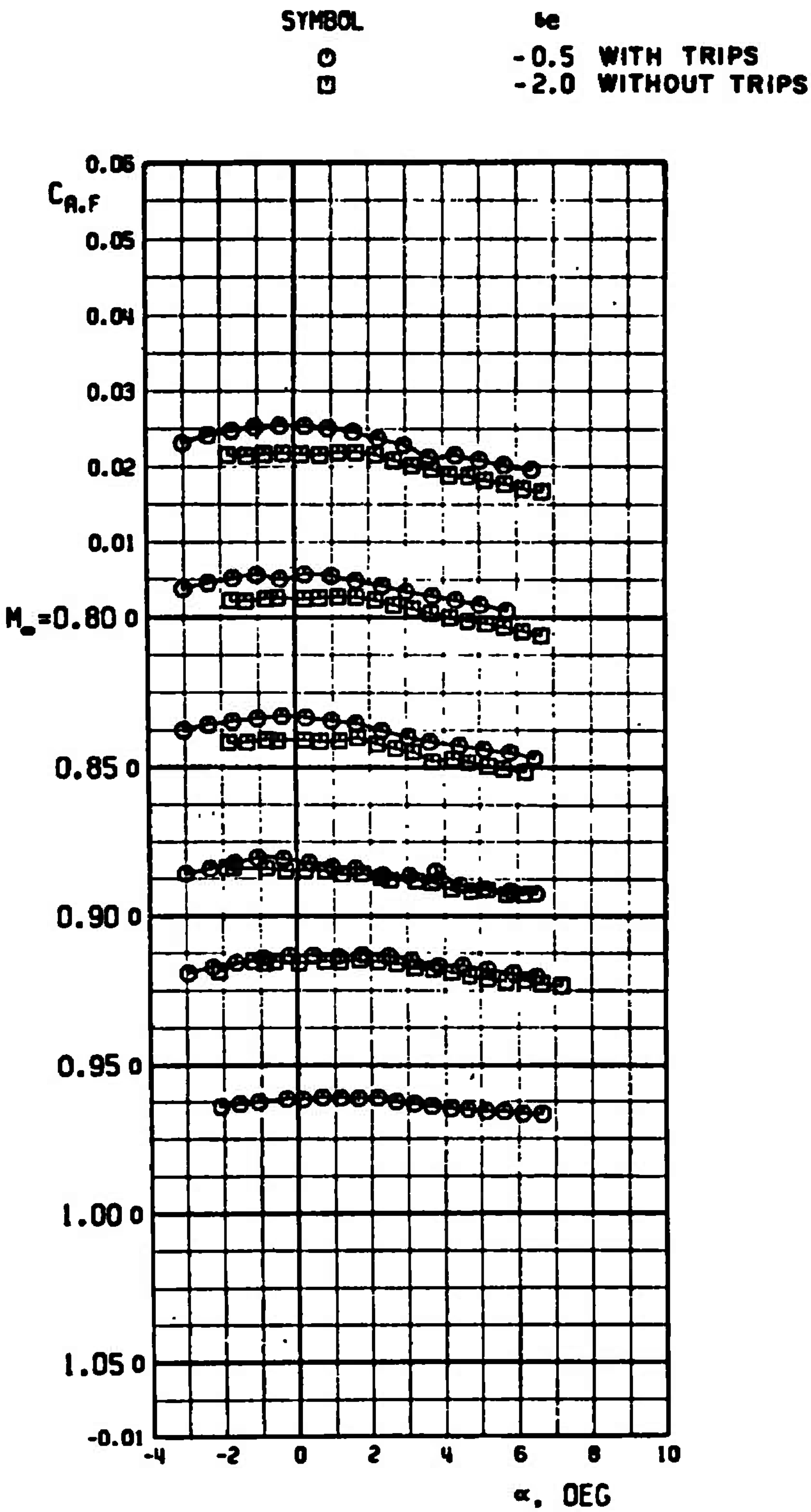

c. Continued
Fig. 4 Continued

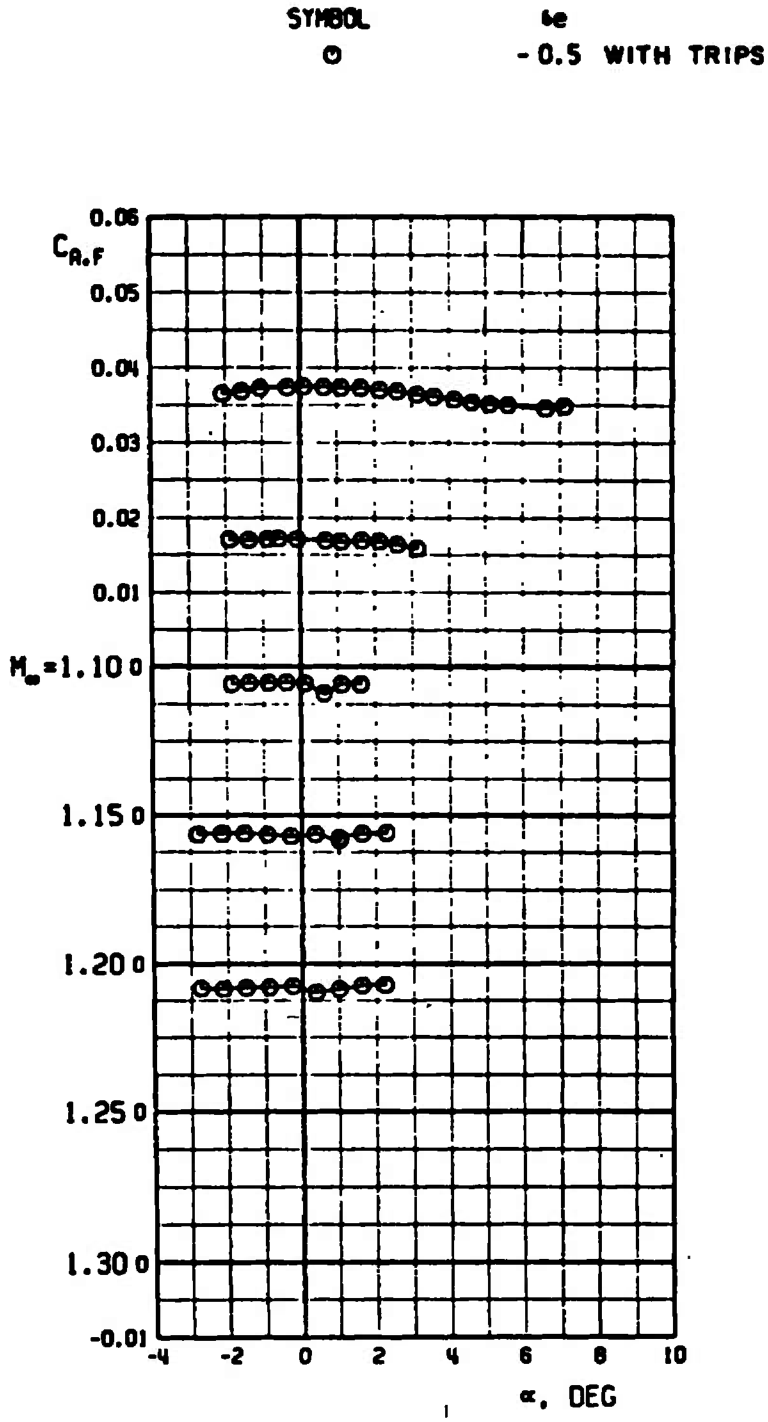

c. Concluded
Fig. 4 Concluded

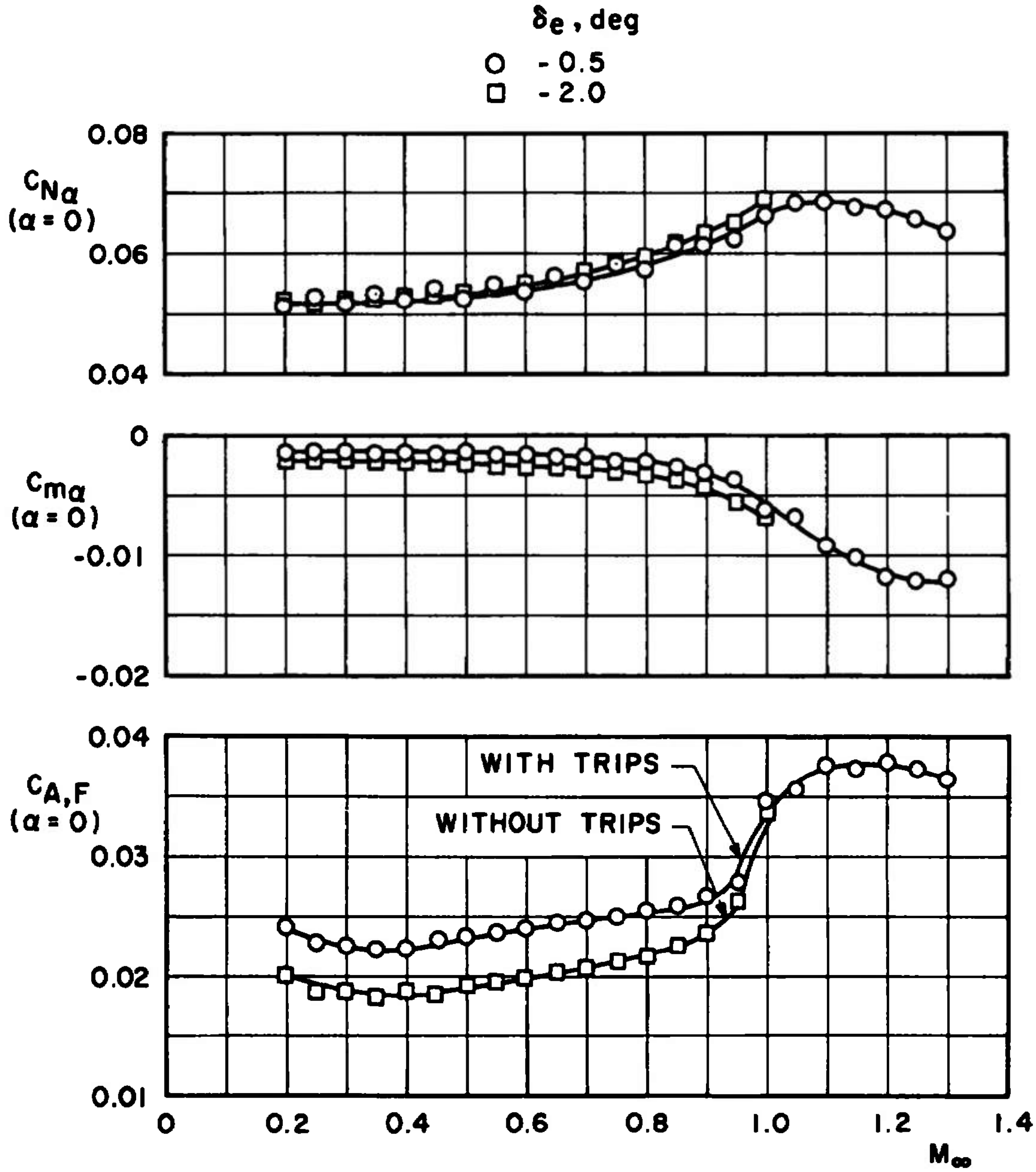

Fig. 5 Variation of the Longitudinal Stability Derivatives and Axial-Force Coefficients at Zero Angle of Attack with Mach Number, $\beta = 0$

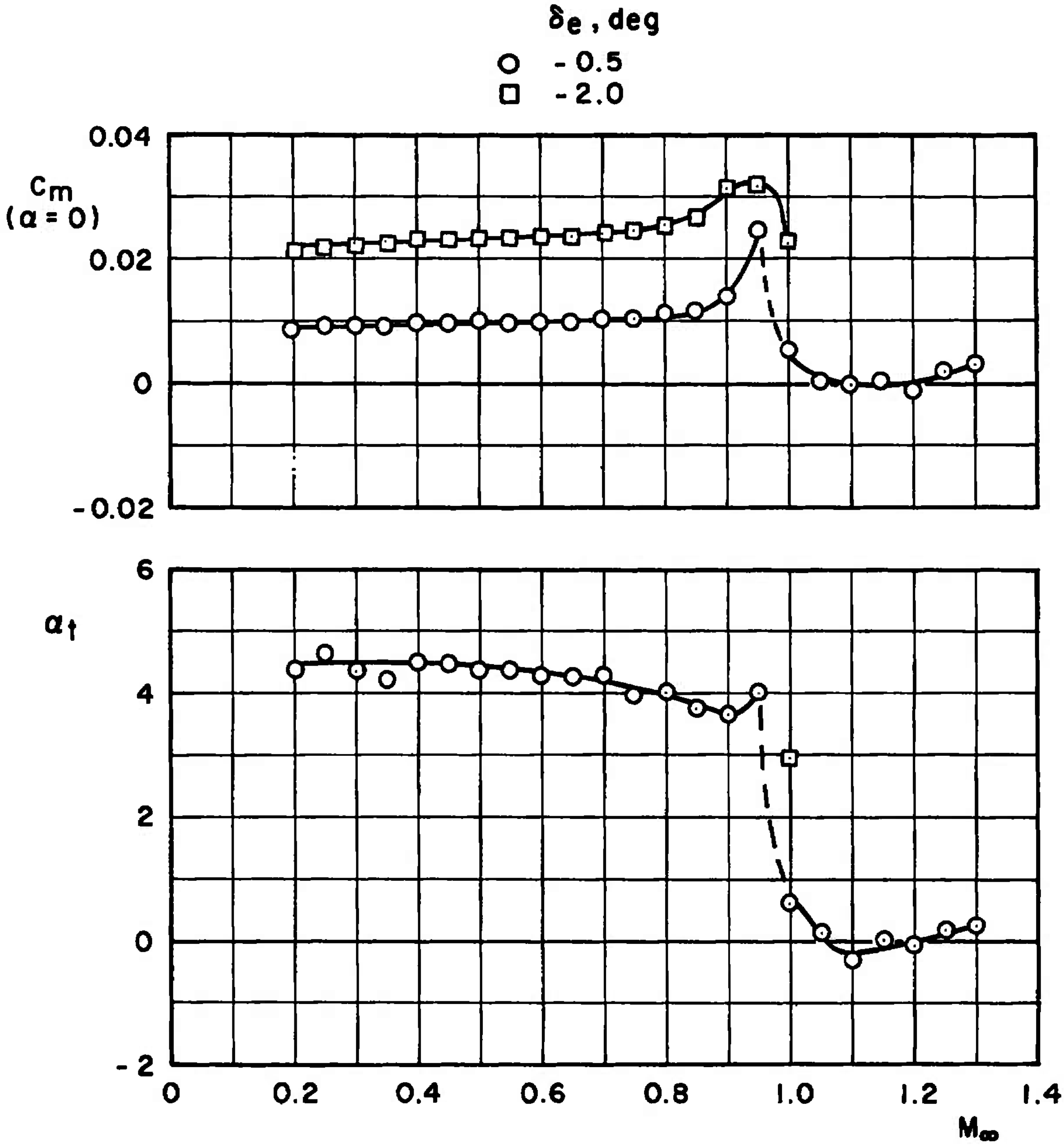

Fig. 6 Effects of Horizontal Tail Deflection on the Pitching-Moment and Trim Characteristics, β = 0

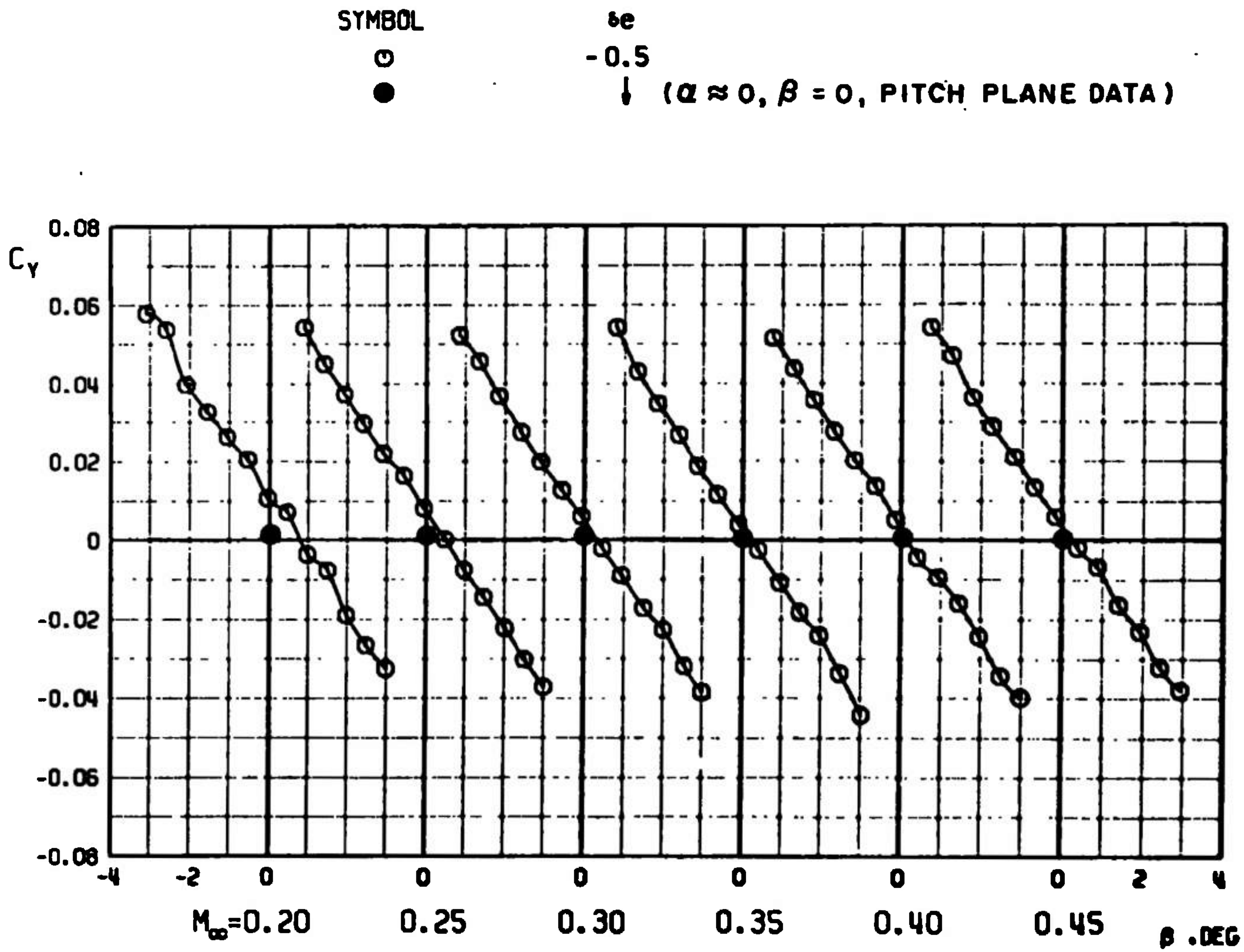

a. C_Y versus β

Fig. 7 Variation of the Lateral Stability and Axial-Force Characteristics with Angle of Sideslip, $\alpha = 0$

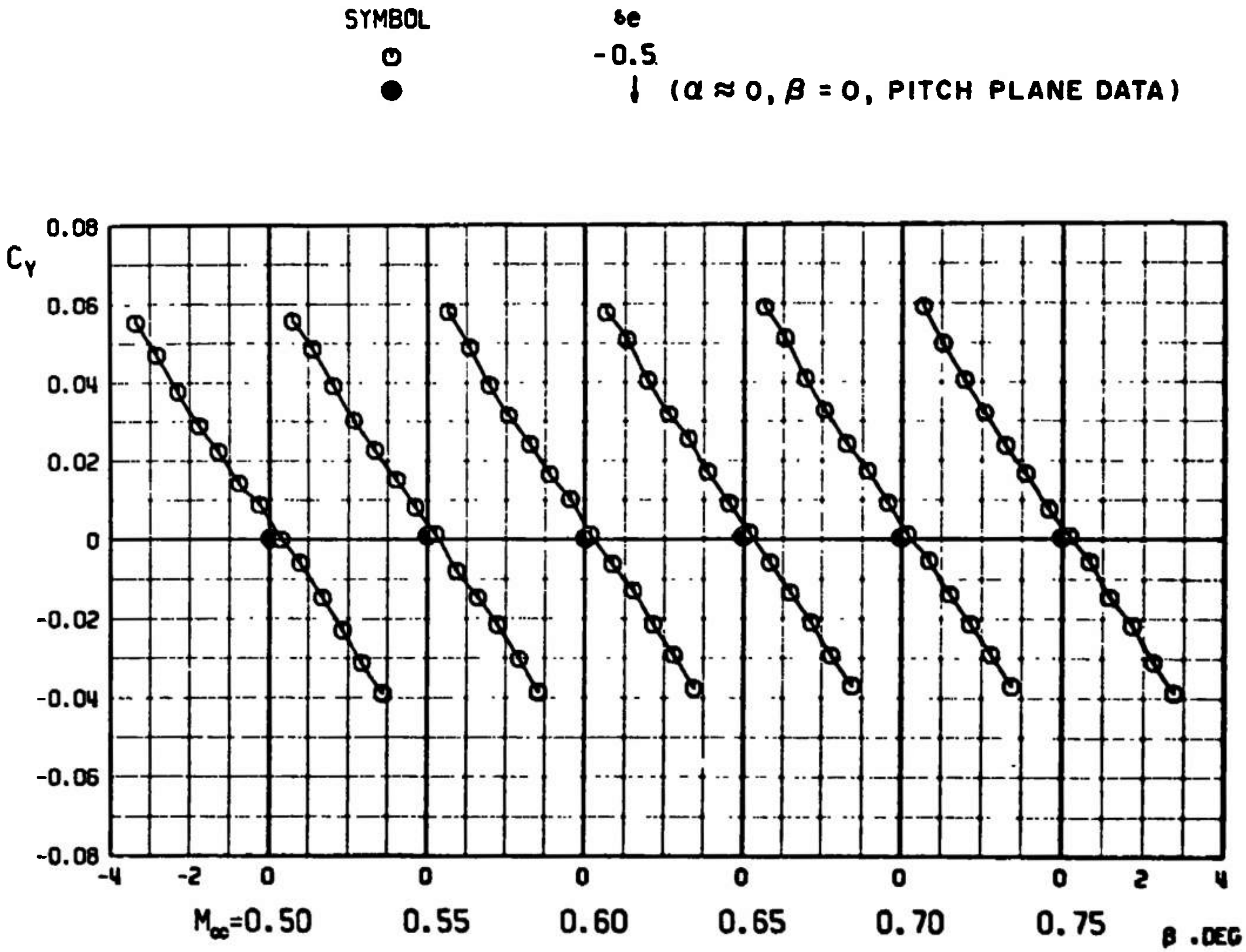

a. Continued
Fig. 7 Continued

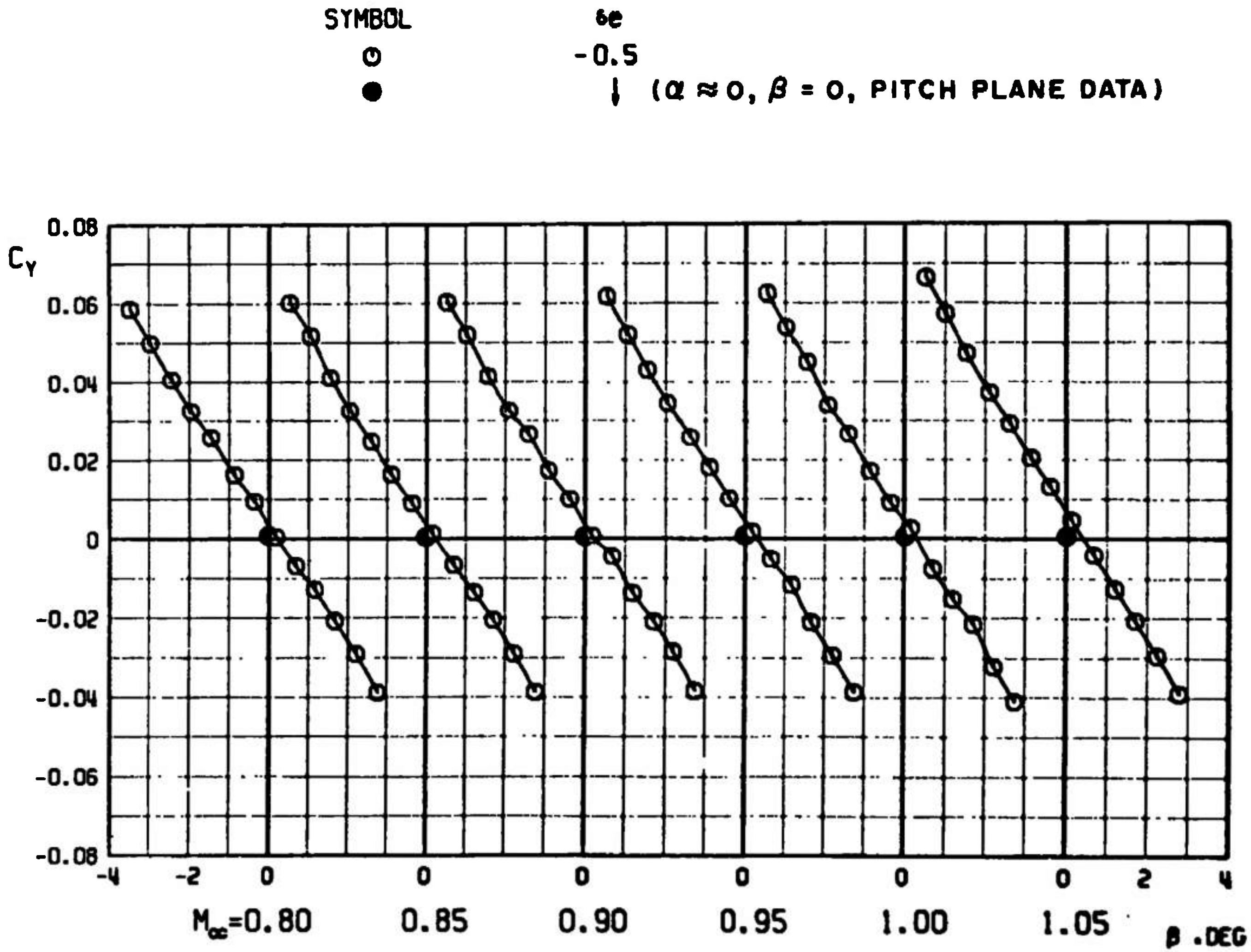

a. Continued
Fig. 7 Continued

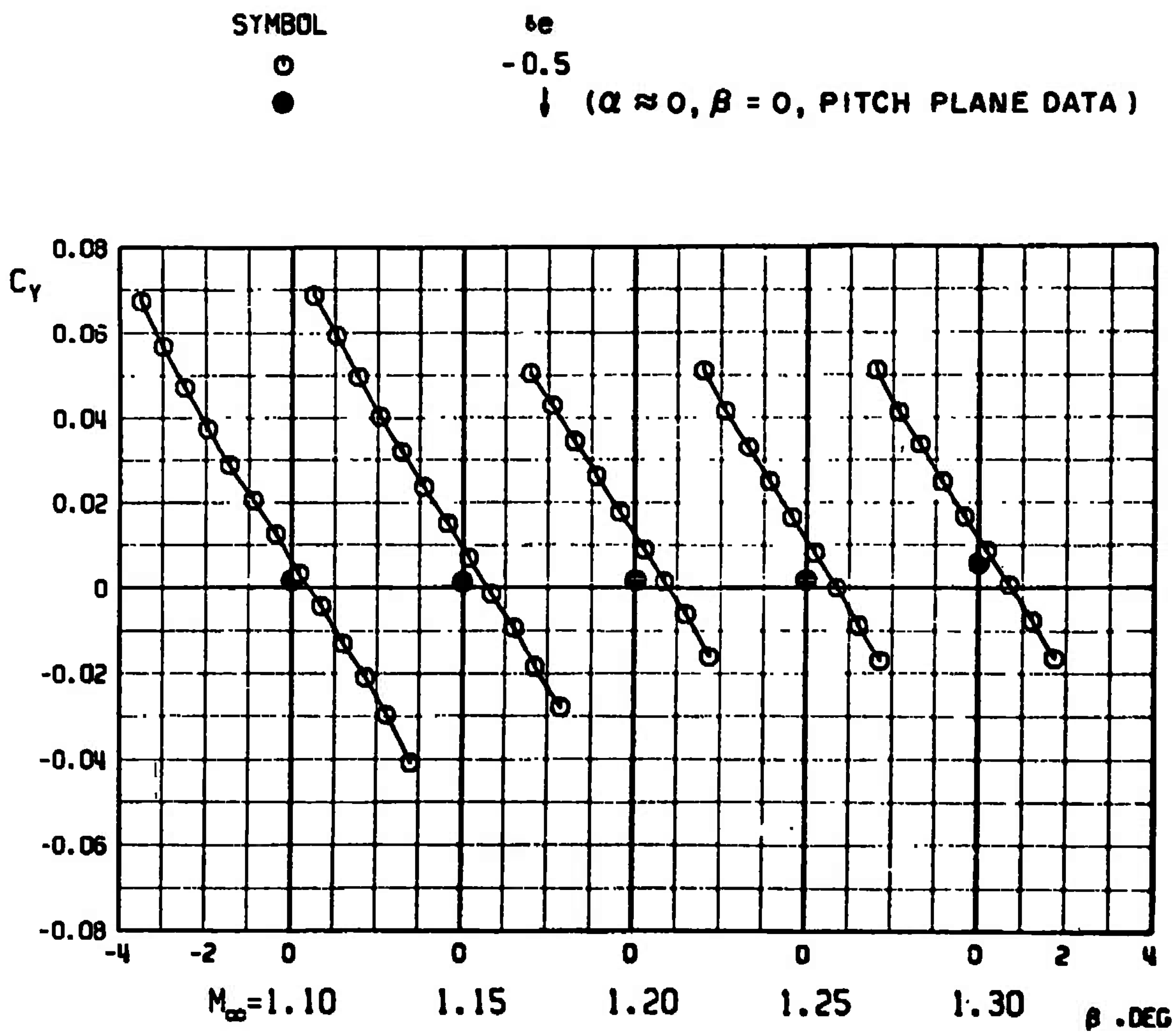

a. Concluded
Fig. 7 Continued

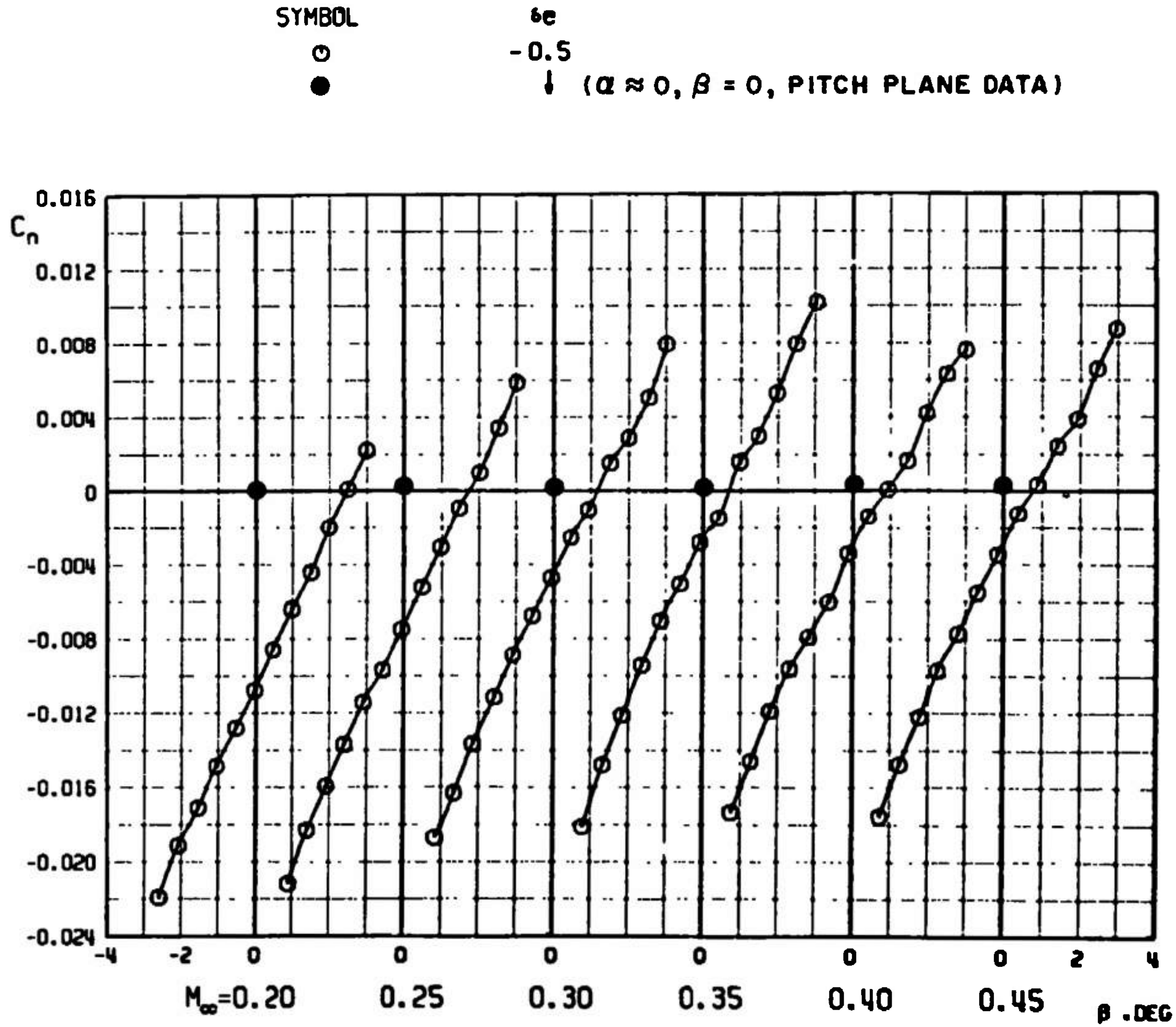

b. C_n versus β
Fig. 7 Continued

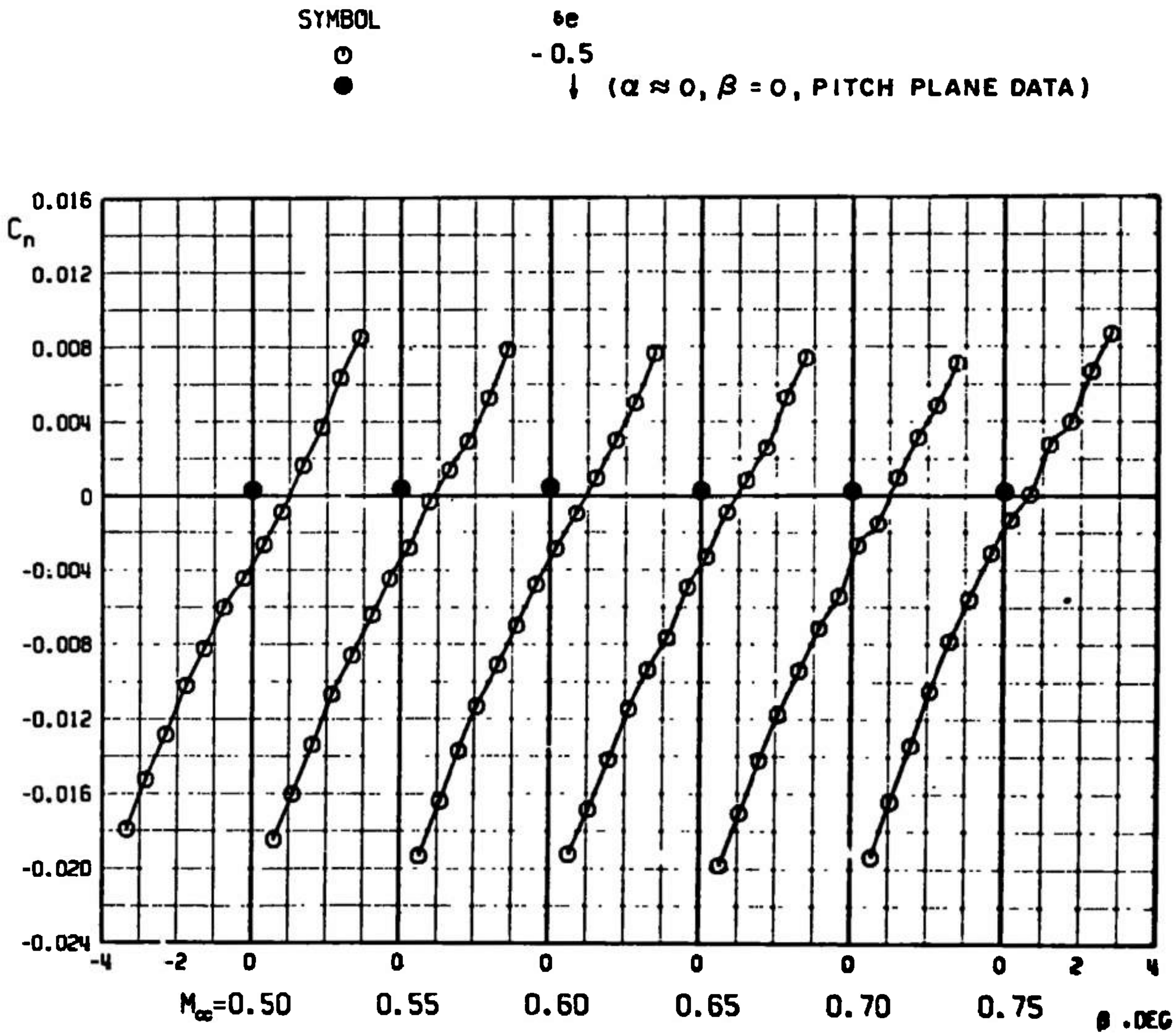

b. Continued
Fig. 7 Continued

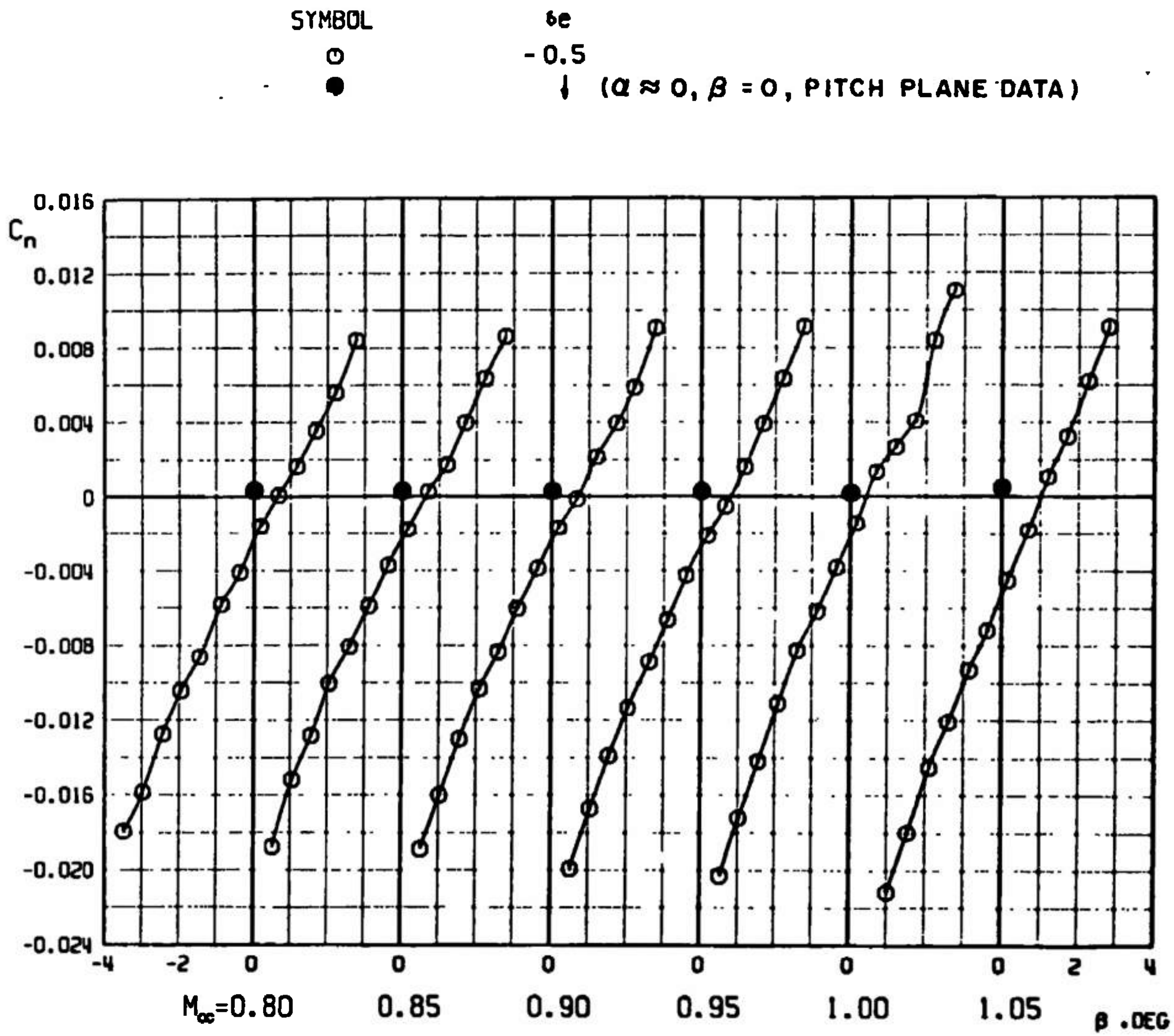

b. Continued
Fig. 7 Continued

SYMBOL	δe	
○	-0.5	
●	↓	($\alpha \approx 0$, $\beta = 0$, PITCH PLANE DATA)

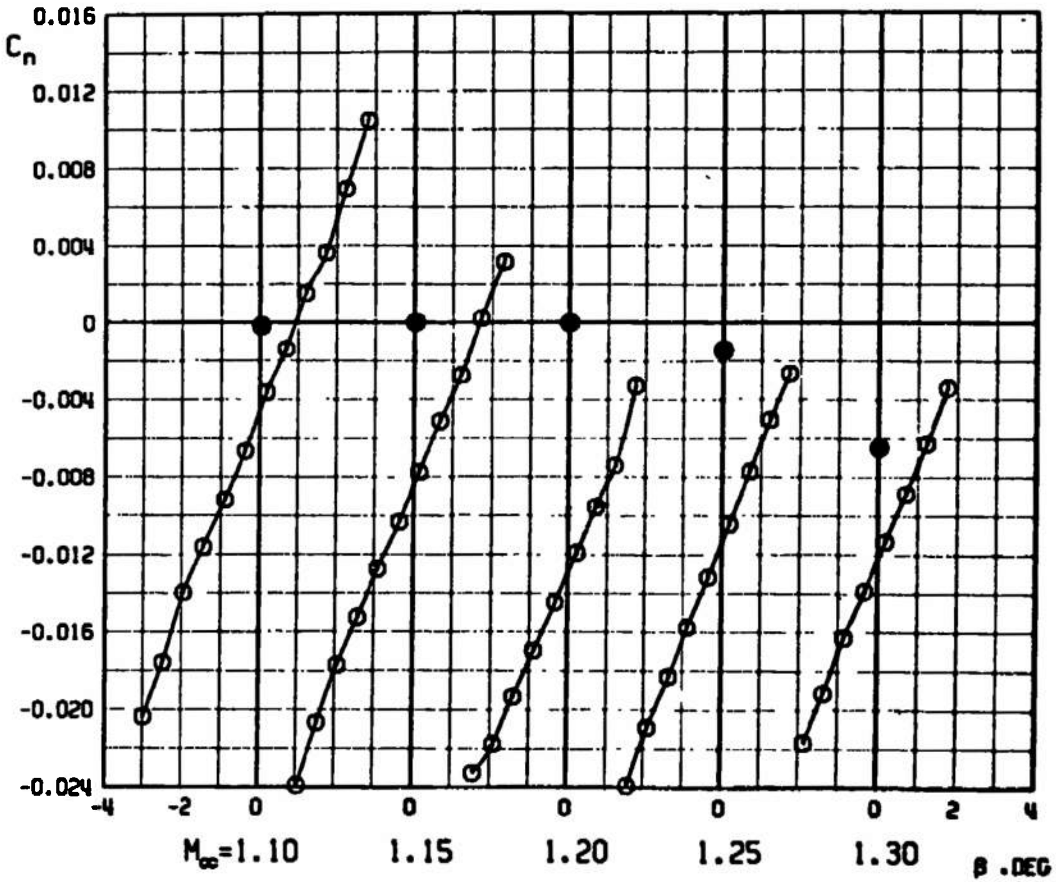

b. Concluded
Fig. 7 Continued

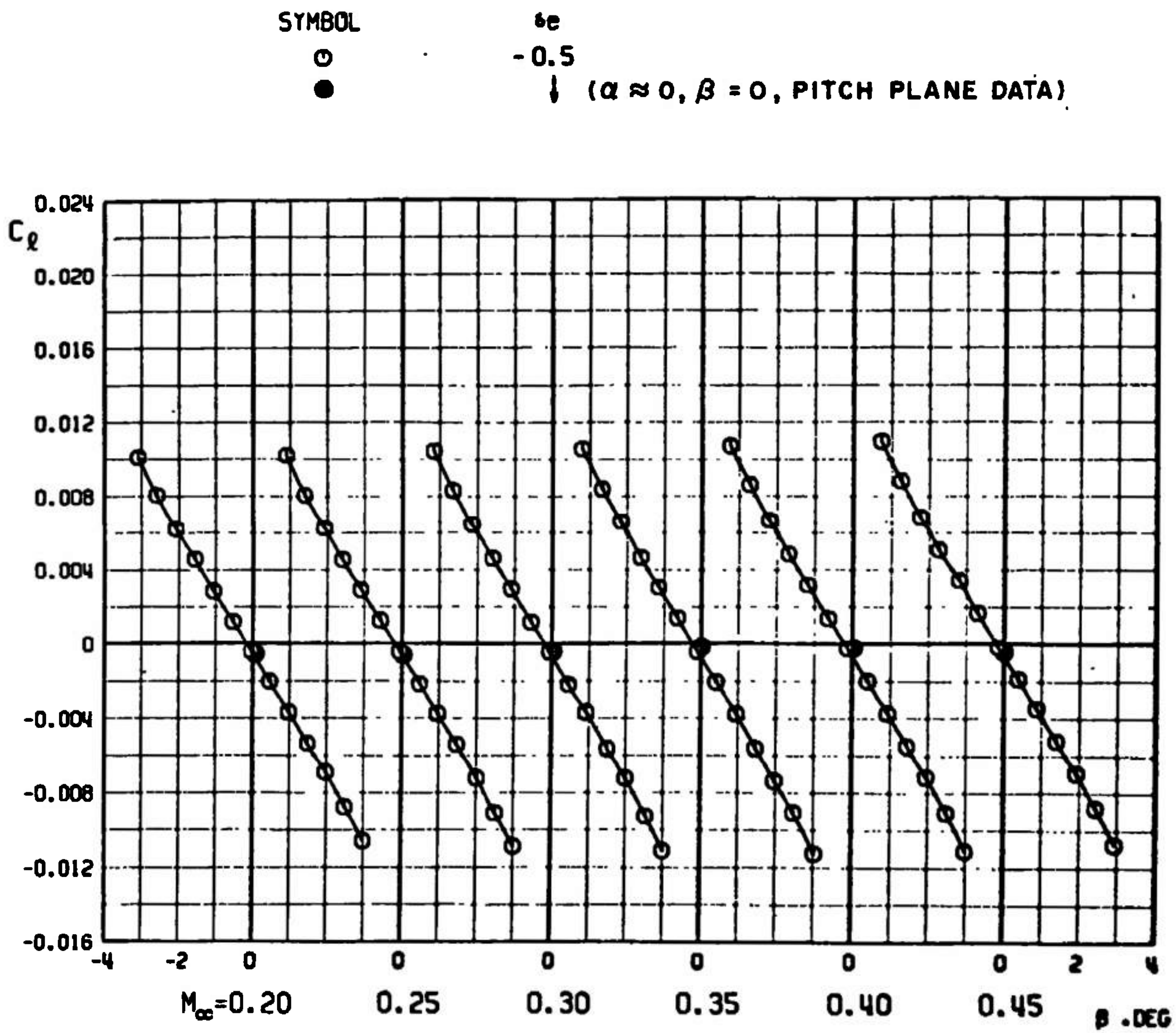

c. C_ℓ versus β

Fig. 7 Continued

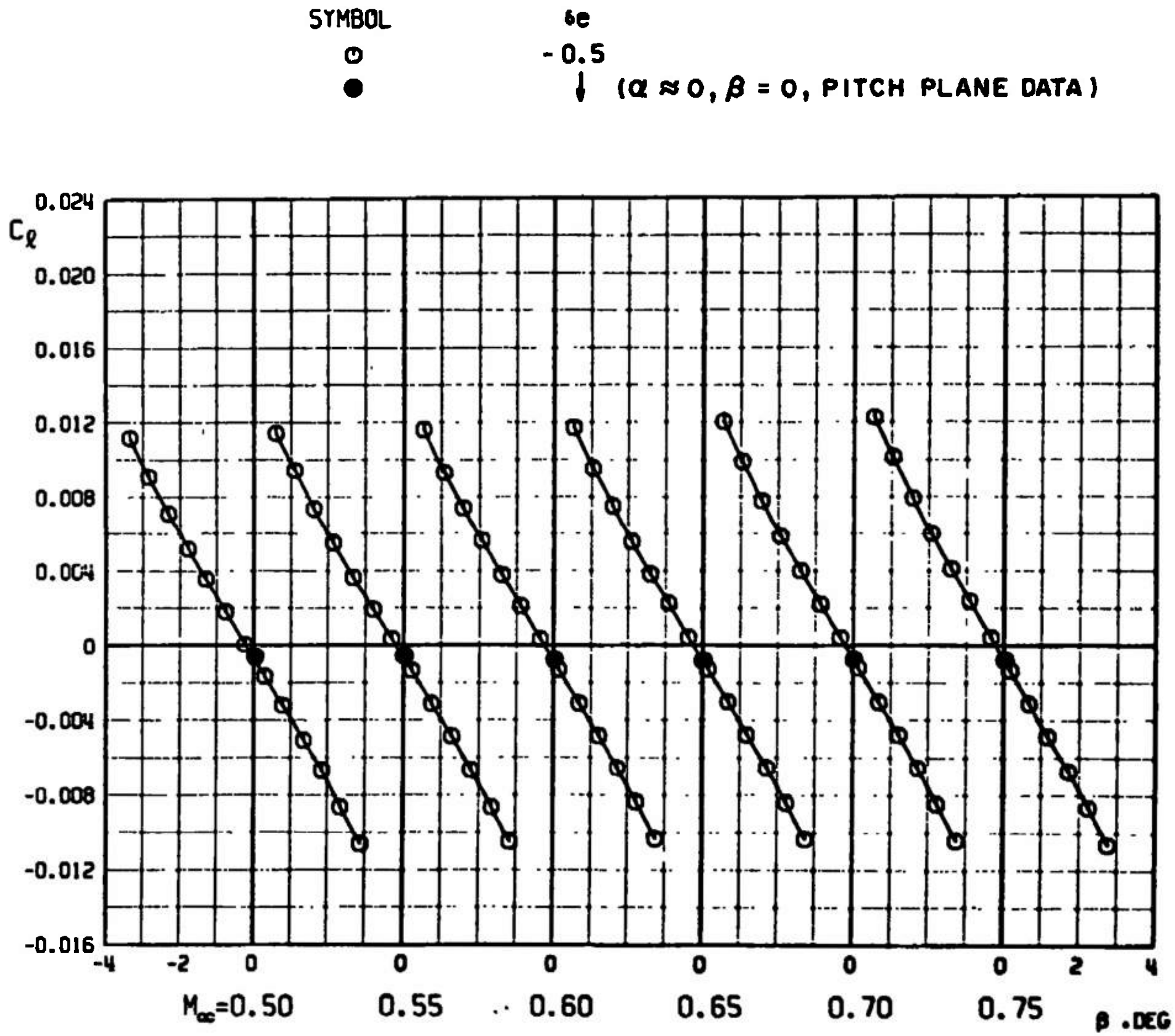

c. Continued
Fig. 7 Continued

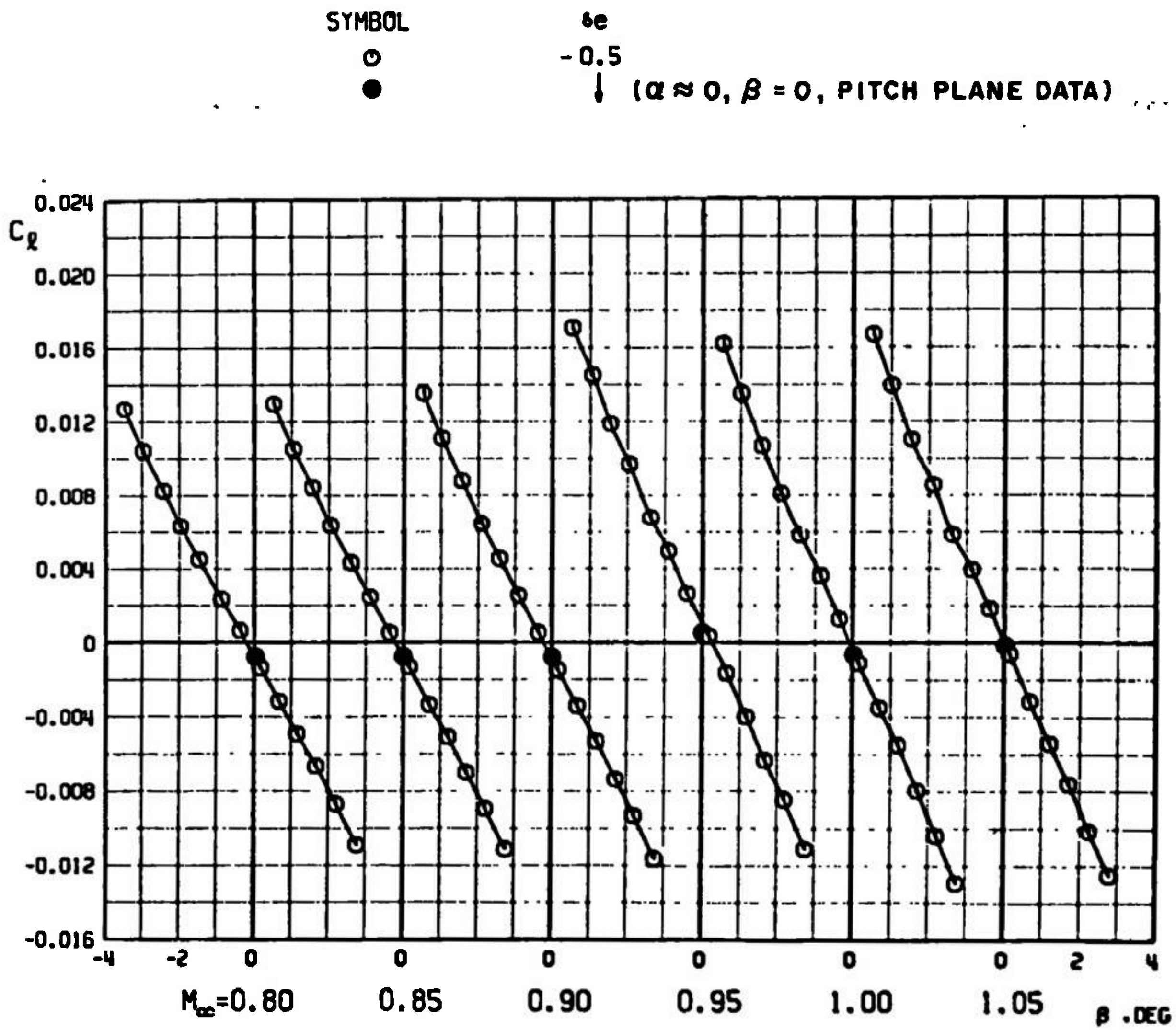

c. Continued
Fig. 7 Continued

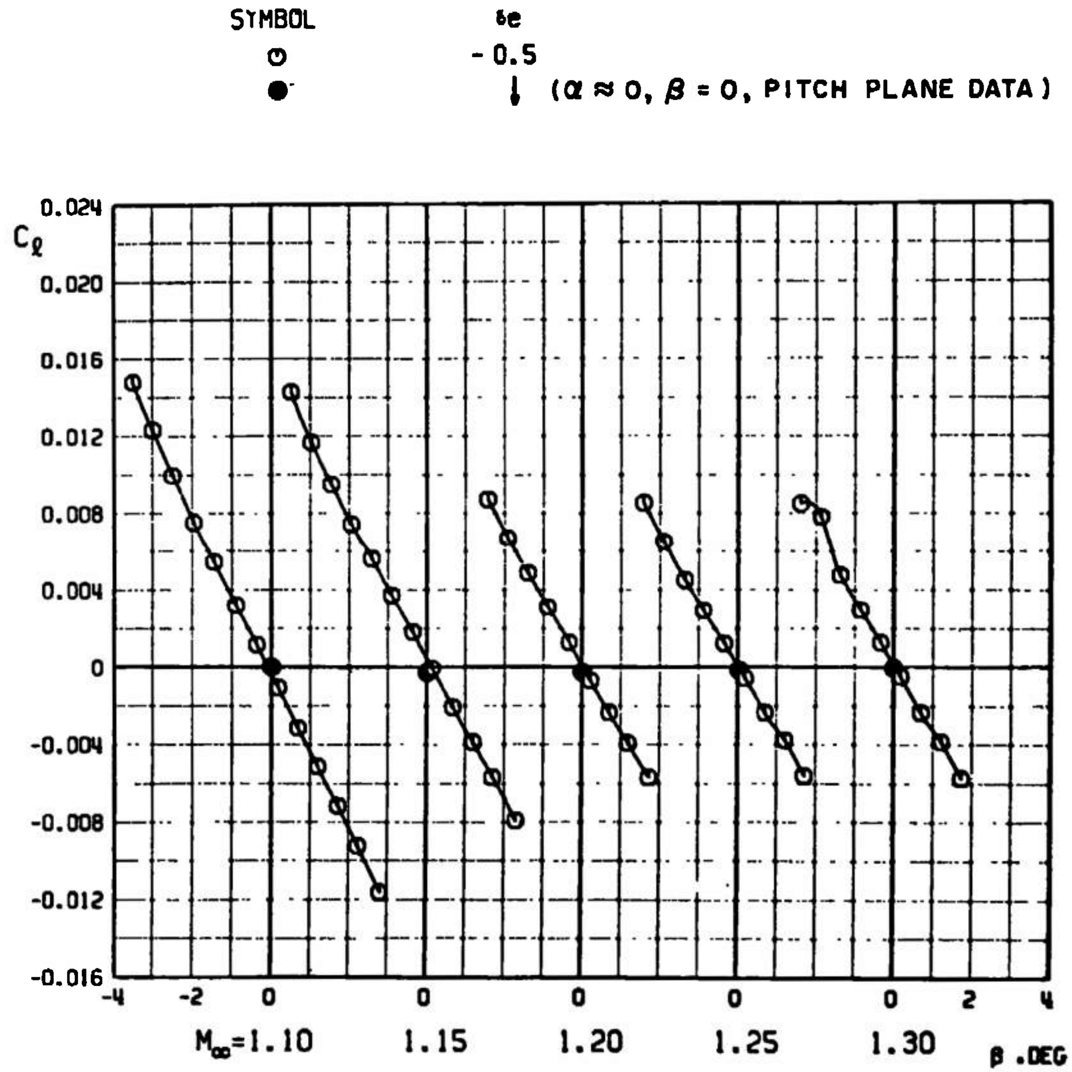

c. Concluded
Fig. 7 Continued

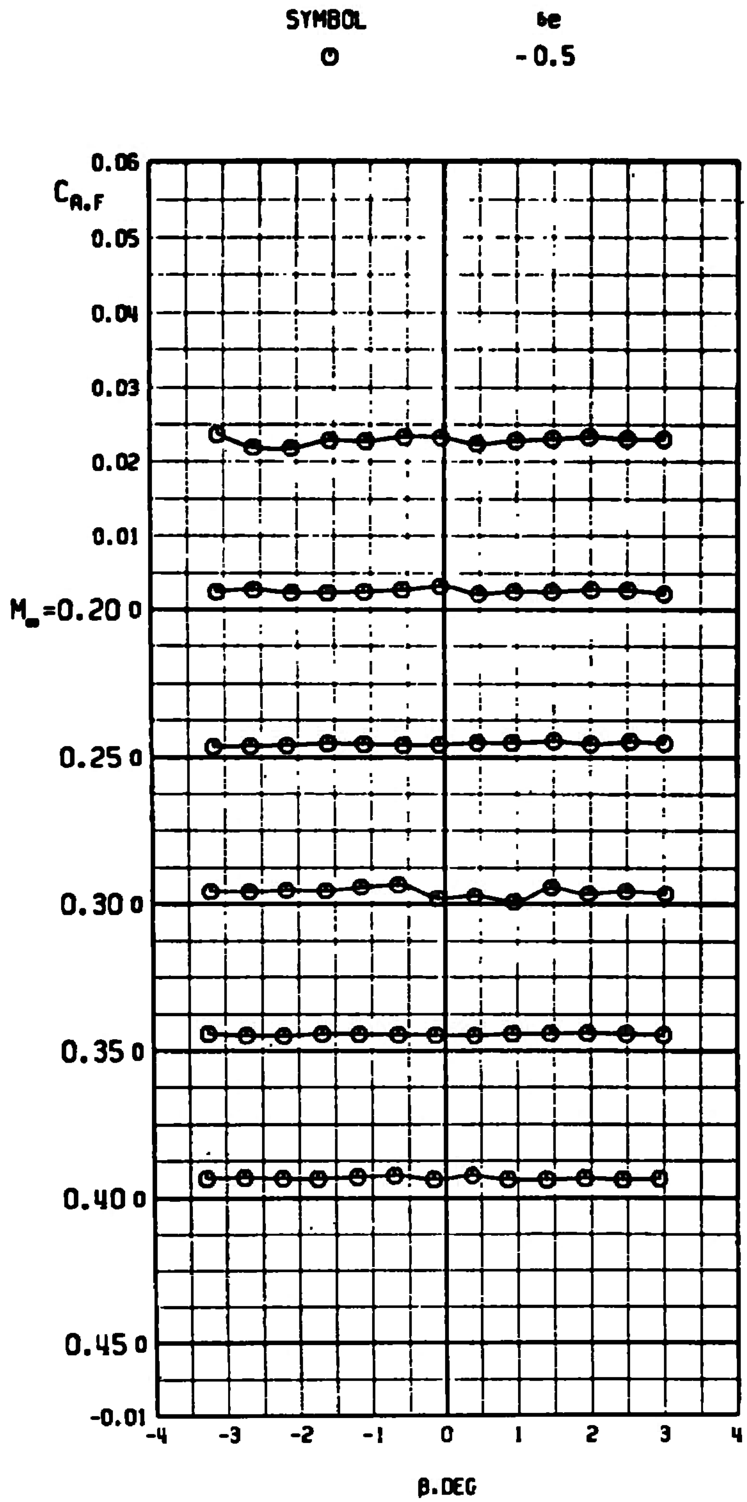

d. $C_{A,F}$ versus β
Fig. 7 Continued

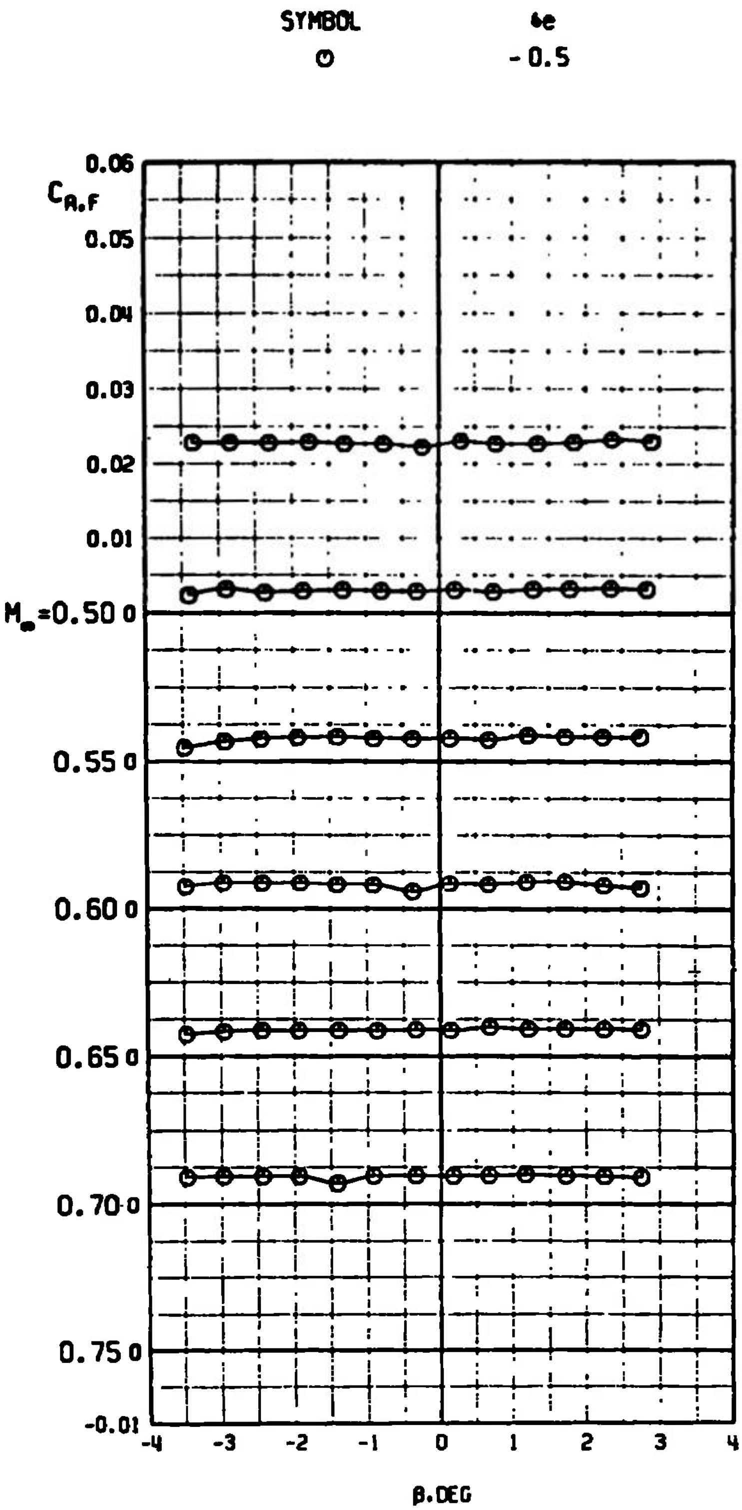

d. Continued
Fig. 7 Continued

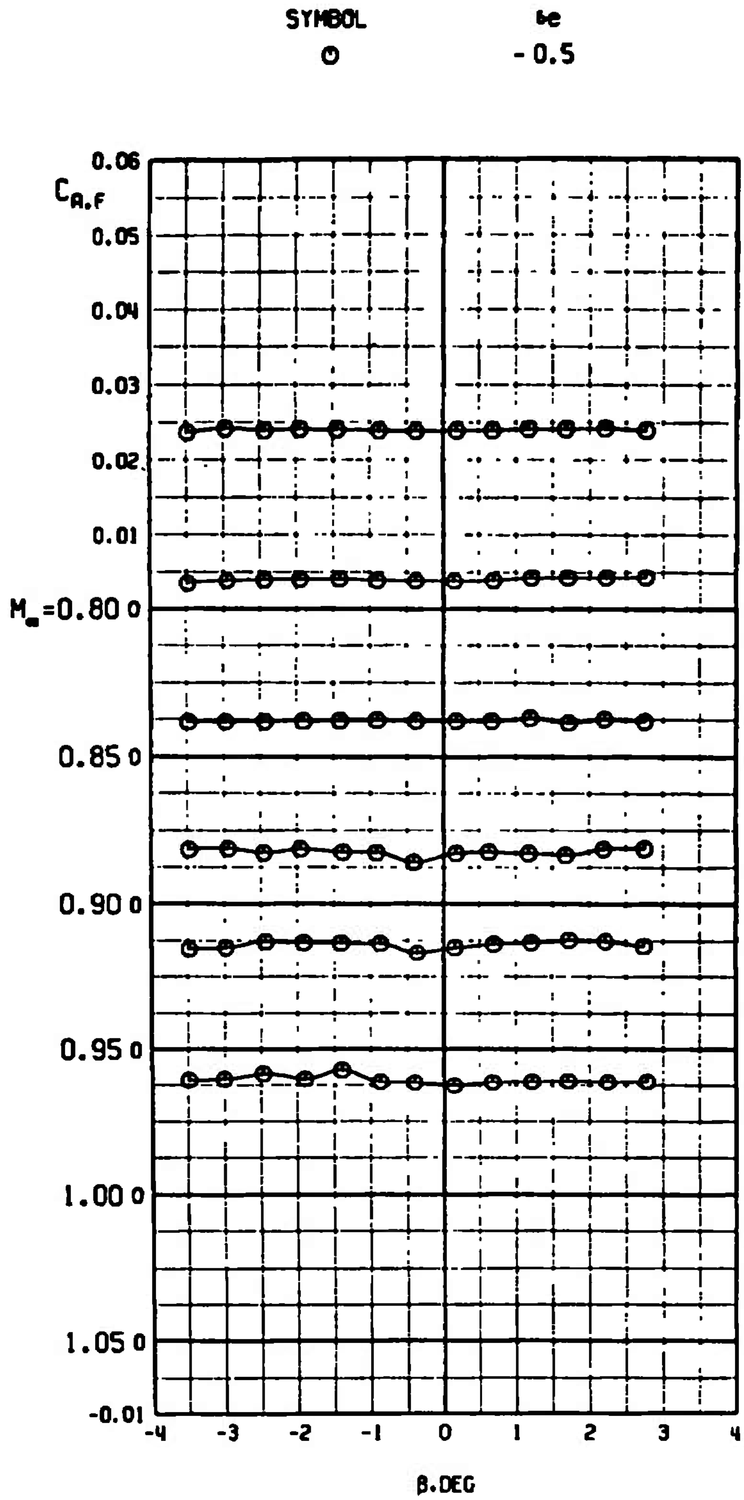

d. Continued
Fig. 7 Continued

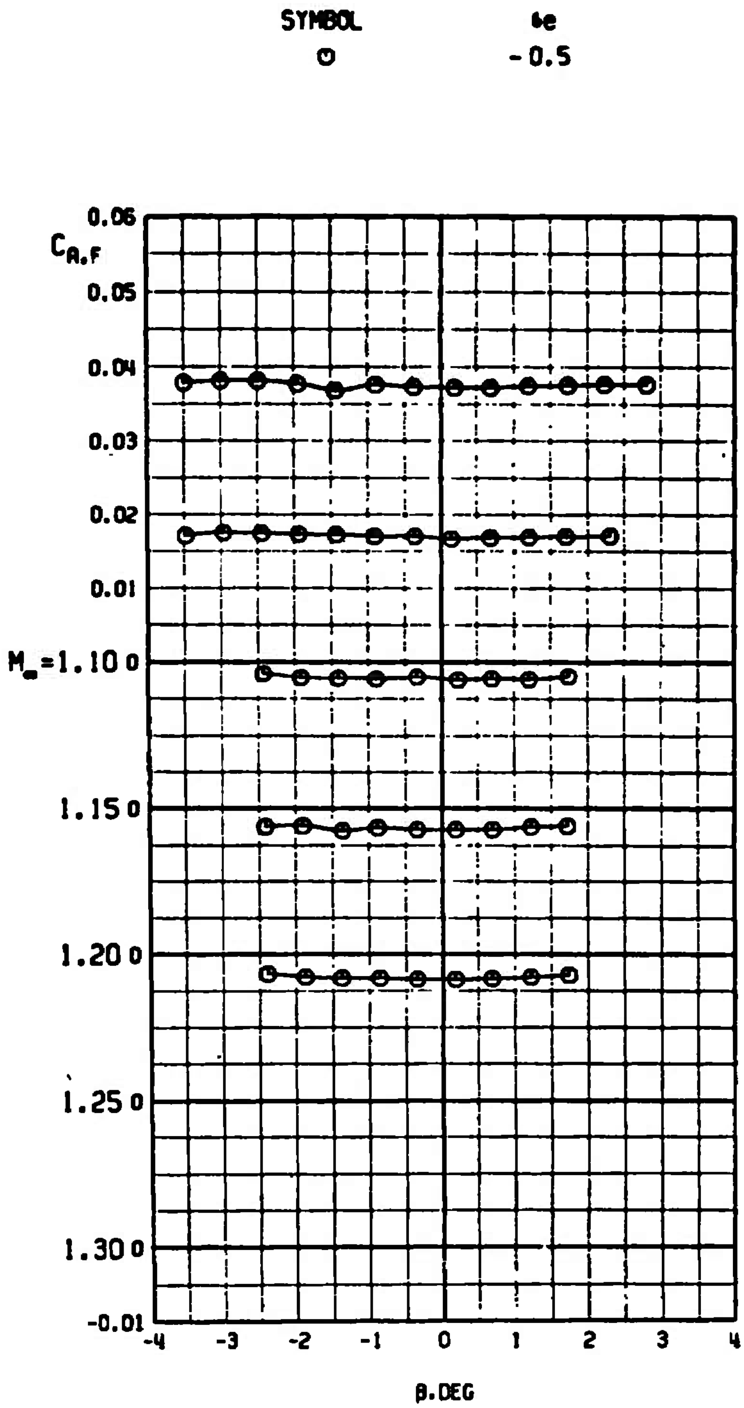

d. Concluded
Fig. 7 Concluded

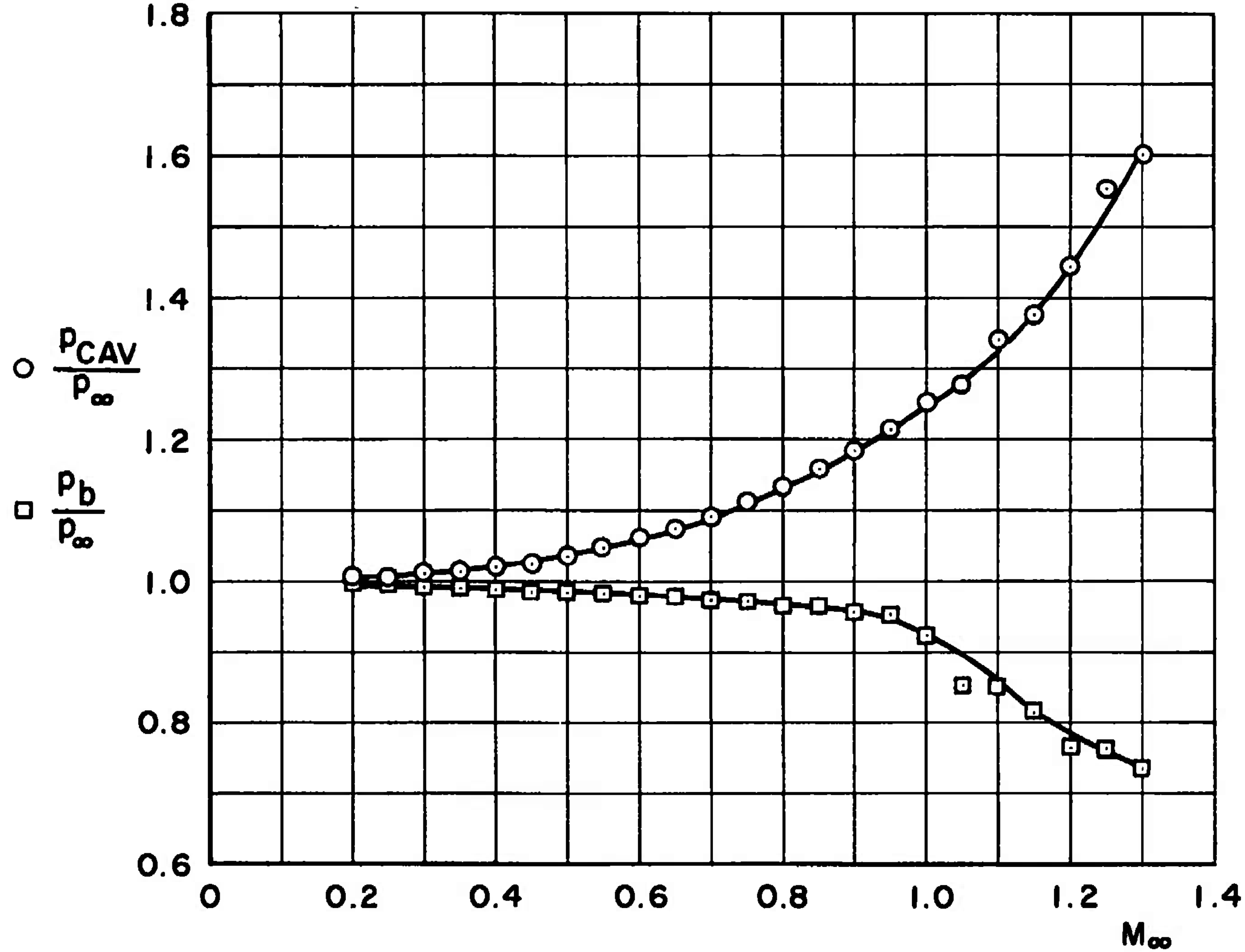

Fig. 8 Variation of the Model Cavity and Base Pressure Ratios with Mach Number

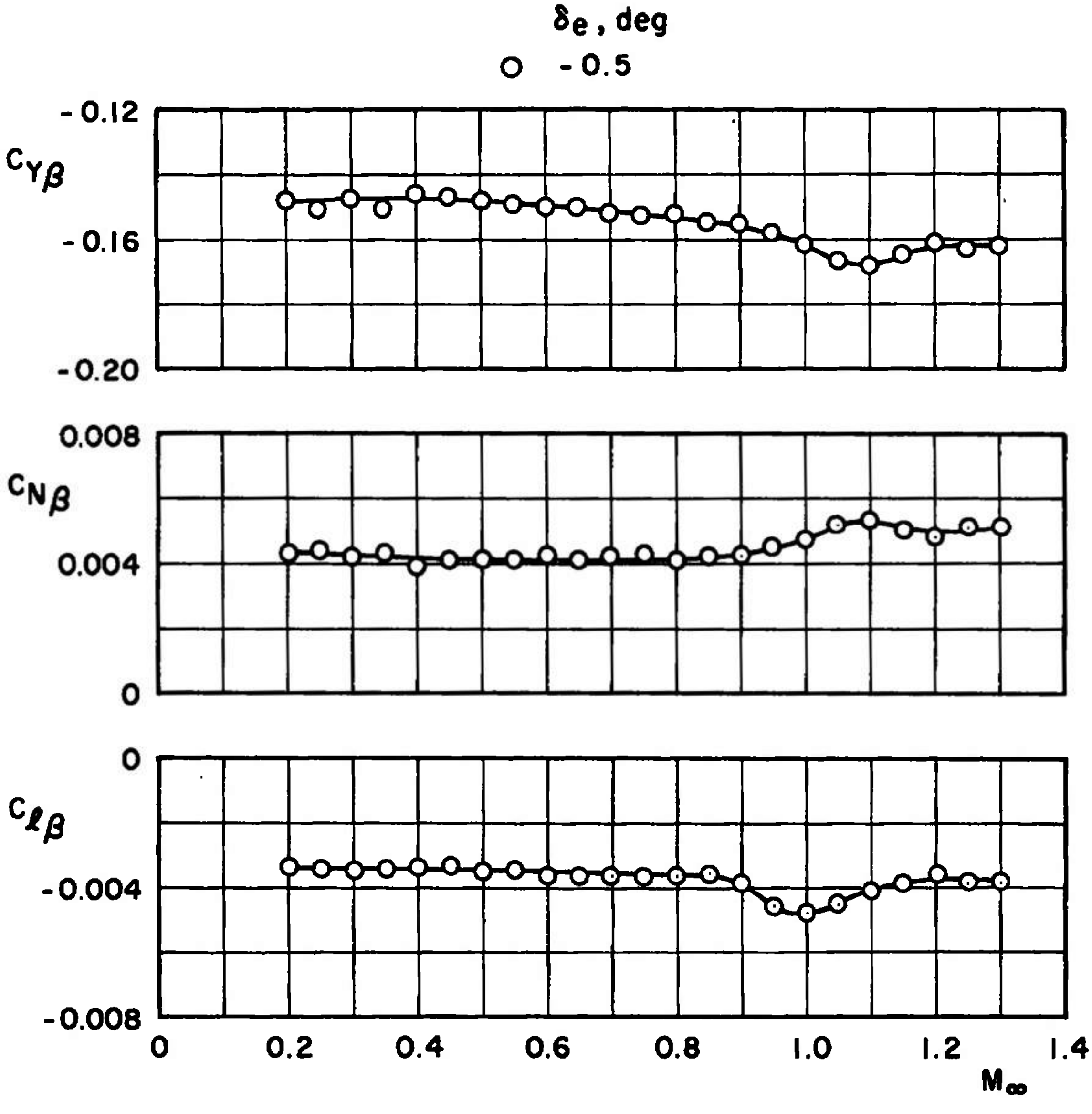

Fig. 9 Variation of the Lateral Stability Derivatives at Zero Angle of Sideslip with Mach Number, $\alpha = 0$

TABLE I
WIND TUNNEL TEST CONDITIONS

M_∞	p_t, psf	T_t, °R	q_∞, psf	p_∞, psf	$Re_\ell \times 10^{-6}$
0.20	3400	540	90	3310	1.50
0.25			140	3260	1.80
0.30			200	3200	2.20
0.35	3020		240	2770	2.20
0.40	2400			2150	2.00
0.45	1920			1670	1.80
0.50	1600			1350	1.60
0.55	1400			1140	1.60
0.60	1200			940	1.40
0.65	1080			810	1.40
0.70	960			690	1.30
0.75	880			600	1.20
0.80	820			540	1.20
0.85	770			480	1.10
0.90	720			430	1.10
0.95	680			380	1.00
1.00	650			340	1.00
1.05	750		290	370	1.20
1.10	710		280	330	1.10
1.15	710		290	310	1.10
1.20	670		280	280	1.10
1.25	540		230	210	0.90
1.30	540		230	200	0.90

TABLE II
TEST SUMMARY

M_∞	δ_e, deg		
	-0.5	-0.5	-2.0
0.20	α = -2 to 8	β = -3 to 3	α = -2 to 8
0.25			
0.30			
0.35			
0.40			
0.45			
0.50			
0.55			
0.60			
0.65			
0.70			
0.75			
0.80			
0.85			
0.90			
0.95			
1.00			
1.05			---
1.10			---
1.15			---
1.20			---
1.25			---
1.30			---

UNCLASSIFIED

Security Classification

DOCUMENT CONTROL DATA - R & D

(Security classification of title, body of abstract and indexing annotation must be entered when the overall report is classified)

1 ORIGINATING ACTIVITY (Corporate author) Arnold Engineering Development Center Arnold Air Force Station, Tennessee 37389	2a. REPORT SECURITY CLASSIFICATION UNCLASSIFIED 2b. GROUP N/A

3 REPORT TITLE

STATIC STABILITY AND DRAG CHARACTERISTICS OF A LOW COST FULL-SCALE TARGET AT MACH NUMBERS FROM 0.2 TO 1.3

4 DESCRIPTIVE NOTES (Type of report and inclusive dates)

Final Report - February 12 through 14, 1973

5 AUTHOR(S) (First name, middle initial, last name)

J. B. Carman, ARO, Inc.

This document has been approved for public release; its distribution is unlimited. Per TAB 76-4 13 Feb, 1976

6 REPORT DATE	7a. TOTAL NO OF PAGES	7b. NO OF REFS
April 1973	55	2

8a. CONTRACT OR GRANT NO b. PROJECT NO 1920 c. Program Element 62602F d.	9a. ORIGINATOR'S REPORT NUMBER(S) AEDC-TR-73-84 AFATL-TR-73-100 9b. OTHER REPORT NO(S) (Any other numbers that may be assigned this report) ARO-PWT-TR-73-42

10 DISTRIBUTION STATEMENT ~~Distribution limited to U.S. Government agencies only; this report contains information on test and evaluation of military hardware; April 1973; other requests for this document must be referred to Air Force Armament Laboratory (AFATL/DLQC), Eglin AFB, FL 32542.~~

11 SUPPLEMENTARY NOTES Available in DDC	12 SPONSORING MILITARY ACTIVITY Air Force Armament Laboratory (AFATL/DLQC) Eglin AFB, FL 32542

13 ABSTRACT

The static stability and drag characteristics were investigated for a 0.05-scale model of a Low Cost Full-Scale Target (LCFST) at Mach numbers from 0.2 to 1.3. Free-stream Reynolds number, based on the mean aerodynamic chord, varied between 0.9 and 2.2 million for angles of attack and sideslip of -2 to 8 deg and -3 to 3 deg, respectively. Data were obtained for horizontal tail deflections of -0.5 and -2 deg. Test results indicated that the target vehicle was statically stable in both the pitch and yaw planes. Negative deflection of the horizontal tail produced a substantial increase in pitching-moment coefficient at $\alpha = 0$.

~~Distribution limited to U.S. Government agencies only; this report contains information on test and evaluation of military hardware; April 1973; other requests for this document must be referred to Air Force Armament Laboratory (AFATL/DLQC), Eglin AFB, FL 32542.~~

DD FORM 1 NOV 65 1473

UNCLASSIFIED

Security Classification

14. KEY WORDS	LINK A		LINK B		LINK C	
	ROLE	WT	ROLE	WT	ROLE	WT
Low Cost Full-Scale Target						
delta wings						
aircraft						
targets						
transonic flow						
static stability						
drag						
wind tunnel tests						

AFSC
Arnold AFS Tenn